Space-frequency distributions in the analysis and modeling of early vision[1]

Gabriel Cristobal[2]

TR-90-046

September, 1990

ABSTRACT

The use of the joint space-spatial frequency representations has recently received considerable attention; specially in those areas of science and engineering where nonstationary signals appear. In that case, local energy distribution representations based in the local spectra computation would be more appropriate. The Wigner Distribution (WD) that gives a joint representation in the space and spatial frequency domain entails a rigorous mathematical framework in the study of these local representations. In this paper, texture recognition is performed through the extraction of features from the WD and a comparative study with other methods is presented.A review of the state-of-the-art of the joint representations in different areasof research, namely signal, speech and vision processing, is presented. Afterwards, the importance of these distributions in the modeling of early vision processes has been considered, presenting a brief review about the physiological findings in order to have a quantitative measure of the degree of biological plausibility.

Keywords: Joint representations, Wigner Distribution, Gabor representation, texture analysis,receptive field modeling.

---

1. An extended version of this paper will appear under the title "Image filtering and analysis through the Wigner Distribution" as a chapter in Advances in Electronics and Electron Physics Series. (Hawkes, P.W., ed), Academic Press, Orlando, Florida.

2. International Computer Science Institute and EE-CS Dept. UC Berkeley. Internet CSNet address: gabriel@icsi.berkeley.edu

Research supported by a Spanish Ministry of Education fellowship.

I. Introduction

The joint space-spatial frequency representations have received special attention in the field of image processing, vision and pattern recognition. This interest is due in essence to three different aspects: this class of functions display all image information in the conjoint domain where the representation is defined; neurophysiological studies have suggested that some cells of the primary visual cortex serve to encode some particular joint representation (Jacobson 1988); and moreover, they have a high pattern separability. Nevertheless, the joint representations must observe some conditions in order to be useful in those areas: the correct marginal distributions should be contained for them, that is, the projections of the representation on the conjoint domain must yield the local image power and the image spectrum; they also should have high resolution in both domains; and they must be positive, in order to be interpreted as an energy distribution onto the joint space-spatial frequency domain. On the other hand, the condition of bilinearity is a logical one in the context of image processing. It has been claimed that the Wigner distribution function (WD) has the best properties to be used in image processing, against other joint representations of this kind. Thus, it has the best resolution, which is matched to that of the image in both domains; it overcomes the resolution trade-offs that traditionally have limited the utility of windowed power spectrum analysis. And besides, the WD is a joint bilinear representation, very close to be positive, invariant within linear transformations, and it contains all image information. These aspects will be explained more extensively below.

In Section II, the definition and properties of the WD for continuous functions have been considered. However, an exact evaluation of this distribution is generally impossible. This is so because the WD is defined, as it will see, by an infinite integral. There are two ways to deal this problem: by computing optically the integral, or by converting the continuous function into a discrete function, and defining discrete versions of the distribution. Then, a discrete version of this distribution is presented, and the consequences of this discretization are discussed. At the end of the second section, the space (time)-frequency distributions are discussed by using the Cohen's unified approach. And the WD's interference problems, introduced by the bilinear definition, are discussed in the context of pattern recognition and image analysis applications.

It has been said above that the WD can be computed analogically, or via digital. In Section II, different implementations of this distribution are presented. First, digital implementations are described in the case of images with 1-D and 2-D variations. The 2-D case could be considered a generalization of the 1-D one, but it will imply excessive number of calculations and high storage requirements. The WD has been computed through the different implementations. And, the

inversion property was tested by recovering the image information.

From the point of view of image processing, it is very interesting that such kind of representation retains all image information, since in this case this information could be retrieved, and the WD meets this property. This suggests to use it in different image processing operations. Nevertheless, it is necessary before its use to estimate the computer requirements that the generation processing, and inversion of the distribution of an image implies. This evaluation bring out the need of developing another class of Wigner processors, that in some case reduce those resources. The hybrid processors take advantages of the best characteristics of the optical and digital processors. In Section III.E, the interest of using VLSI technology in the generation of the joint representations, and in particular the WD, has been considered.

Although an increasing corpus of evidence suggests the mammalian biological visual systems are capable to a selective spatial frequency analysis, however the use of the classical Fourier spectra to texture analysis have been partially successful (Sutton 1972, Weszka 1976). The main reason for these dishearten results is due to the fact each frequency component contents global information. On the other hand, the shift-invariance property of the Fourier spectra is obtained at expense of the loss of phase information. However, as Oppenheim and Lim have demonstrated many features of a signal are retained in the phase information but not in the amplitude (Oppenheim 1981). This fact led to some researchers to consider the use of local image representations by computing the power spectrum over subregions of an image. Bajcsy and Libermann were the first to perform work in this area using local (windowed) measurements of the image spectrum to compute the texture gradient (Bajcsy 1976). The use of space-frequency distributions comes to overcome the shortcomings of the traditional Fourier analysis. Section III deals with the application of the WD for texture discriminations and classification by using both pairwise linear and discriminations analysis. Several textural features have been extracted from the WD and a comparative study with the classical Fourier feature extraction methods has been performed.

In section IV a review of the applications of space (time)-frequency distribution has been presented emphasizing those which are vision oriented. Afterwards, the importance of these distributions in the modeling of the early vision processes has been considered, presenting a brief review about the physiological findings in order to have a quantitative measure of the degree of biological plausibility. Some additional pointers have been included in the References Section for its relationship with the present work.

II. The Wigner Distribution.

A. Definition

The modeling of stationary linear processes, in the area of signal processing, can be done by its spatial (or temporal) amplitude or by its spatial-or temporal- frequency; however the assumption of stationary fails to be true in many applications. In that case, it would be more appropriate to define a local power spectrum that combines the advantages of both descriptions. The Wigner distribution (WD) that gives a joint representation in the space and spatial-frequency domain, entails a rigorous mathematical framework in the study of these local representations. The WD significance and usefulness would be pointed out by means a musical score (Bartelt 1980). The musical score constitutes a fairly good representation for the musician but is erroneous from the mathematical point of view try to specify a monochromatic frequency in a given point of time. It would be necessary to observe the signal at least in a period of time in order to define the frequency of the signal.

The Wigner Distribution (WD) introduced by Wigner (Wigner 1932) as a phase representation in Quantum Mechanics gives a simultaneous representation of a signal in space an spatial-frequency variables. It belongs to a large class of bilinear distributions known as the Cohen's class, in which each member can be obtained choosing different kernels in the generalized bilinear distribution definition (Cohen 1966, Claasen 1980c). The Wigner Distribution might be interpreted as a local or regional spatial frequency representation of an image. It represents two main advantages with respect to other local representations. First, the WD is a real valued function and encodes directly the Fourier phase information. Second, the election of the appropriate window size, which depends on the kind of analyzed information, is not required for the computation of the WD.

The WD of a 2-D image is a 4-D function that involves Fourier transformation for every point of the original image. This fact leads to consider different alternatives to compute the WD of discrete images (see Section II.E). In order to overcome these problems, two possible alternatives has been proposed. First, several hybrid optical-digital image processors have been proposed in the literature to generate the WD of 1-D and 2-D signals. Second, some VLSI special purpose architectures has been recently proposed for computing the distribution.

In this Section, we consider the auto-Wigner distribution function corresponding to 1-D signals for notational simplicity, being the extension to 2-D signals straightforward. Let suppose a continuous, integrable and complex function f(x). The symmetric definition of the Wigner distribution $W_f(x,\omega)$ is given by

$$W_f(x,\omega) = \int_{-\infty}^{\infty} f(x+\frac{x_0}{2}) f^*(x-\frac{x_0}{2})\, e^{-j\omega x_0} dx_0 \tag{2.1}$$

where x and x_0 are spatial variables, ω is the spatial frequency variable and $f^*(\cdot)$ means the complex conjugate of $f(\cdot)$. The *product function* $r_f(x,x_0)$ is given by

$$r_f(x,x_0) = f(x+\frac{x_0}{2}) f^*(x-\frac{x_0}{2}) \tag{2.2}$$

The auto-Wigner distribution gives a generalized autoconvolution at non-zero frequency (Szu 1982). From (2.1), it can be observed that the WD is the Fourier transformation, for a given point x_0, of the image product $f(\cdot)f^*(\cdot)$. It may also be obtained from the Fourier transform, $\mathcal{F}(\cdot)$,of $f(\cdot)$ by

$$W_{\mathcal{F}}(\omega,x) = \int_{-\infty}^{\infty} \mathcal{F}(\omega+\frac{\omega_0}{2})\, \mathcal{F}^*(\omega-\frac{\omega_0}{2})\, e^{j\omega_0 x} d\omega_0 \tag{2.3}$$

According to (2.1) and (2.2) the following relation is observed

$$W_f(x,\omega) = W_F(\omega,x) \tag{2.4}$$

which shows the symmetry between the two conjugate domains (space and spatial-frequency). The mathematical foundations of the WD were considered by De Bruijn in the context of Quantum Mechanics applications (De Bruijn 1973). However they can be modified in many instances to the field of signal processing.

The Wigner Distribution is closely related with the Ambiguity Function (AF) proposed by (Woodward 1953) in the study of radar signals, which definition is given by

$$A_f(\omega,x) = \int_{-\infty}^{\infty} f(x_0+\frac{x}{2}) f^*(x_0-\frac{x}{2})\, e^{-j\omega x_0} dx_0 \tag{2.5}$$

Both Eq. (2.1) and (2.5) could be considered particular occurrences of the generalized local spectral signal representation complex-spectrogram (CS), defined by

$$S_{fg}(x,\omega) = \int_{-\infty}^{\infty} f(x_0+\frac{x}{2})\, g^*(x_0-\frac{x}{2})\, e^{-j\omega x_0} dx_0 \tag{2.6}$$

The CS can be interpreted as a windowed process of the signal f(x) by a shifting window function g(x) (rectangular, gaussian, etc.) and Fourier transforming the product $f(\cdot)g^*(\cdot)$. If the function f(x) is chosen as window g(x), a self-windowed S_{ff} version is obtained in (2.5). In that case, the Eq. (2.5) and (2.6) are equivalent by the following relation

$$A_f(\omega,x) = S_{ff}(x,\omega) \tag{2.7}$$

Comparing Eqs. (3.1) and (3.5) leads to conclude that the Wigner Distribution is related with the Ambiguity Function through a double Fourier Transformation

$$W_f(x,\omega) = \int_{-\infty}^{\infty}\int_{-\infty}^{\infty} A_f(\omega_0,x_0)\, e^{j\omega_0 x} e^{-j\omega x_0} dx_0 d\omega_o \tag{2.8}$$

The AF can be interpreted as a signal autocorrelation in presence of Doppler shifts (Bartelt 1980).

B. Properties

A complete study of the properties of the WD was formulated by (Claasen 1980). The most salient properties for image processing applications are listed below.

1. Realness

The WD of any real or complex function is always real since it is the Fourier transformation of an hermitian product function (see Eq. 2.2). However, it is not possible to interpret this distribution as a density energy distribution, because the WD is not always positive. This implies that the phase information is implicitly encoded in the changes of sign of the distribution. The importance of the Fourier-phase in image representation and analysis has been recognized for different authors (Oppenheim 1981), (Behar 1988). The WD-phase information gives up the spatial dependence correspondent to the spectral frequencies.

2. Space and spatial-frequency marginals

The WD integration over the spatial variable at a fixed frequency gives the spectral energy

density at that frequency, and the WD integration over the frequency variable at a fixed point gives the local power at that point

$$\int_{-\infty}^{\infty} W_f(x, \omega)\, dx = |\mathcal{F}(\omega)|^2 \tag{2.9}$$

$$\frac{1}{2\pi} \int_{-\infty}^{\infty} W_f(x, \omega)\, d\omega = |f(x)|^2 \tag{2.10}$$

3. Finite support

In the case of space-limited signals, the WD is zero out of the range of signal definition. The same property applies to the spatial-frequency domain.

if	f(x)=0	for $\|x\|>N$	
then	$W_f(x,\omega)=0$	for $\|x\|>N$	(2.11)
if	$\mathcal{F}(\omega)=0$	for $\|\omega\|>M$	
then	$W_f(x,\omega)=0$	for $\|\omega\|>M$	(2.12)

4. Space and frequency shifts

Shifts in space and frequency domains give corresponding shifts in the distribution.

$$g(x)=f(x-x_0) \quad \rightarrow \quad W_g(x,\omega)=W_f(x-x_0,\omega) \tag{2.13}$$

$$\mathcal{G}(\omega)=\mathcal{F}(\omega-\omega_0) \quad \rightarrow \quad W_g(x,\omega)=W_f(x,\omega-\omega_0) \tag{2.14}$$

5. Inversion

The product function $r_f(x,x_0)$ (see Eq. 2.2) can be recovered by a inverse Fourier transformation

$$r_f(x, x_0) = \frac{1}{2\pi} \int_{-\infty}^{\infty} W_f(x, \omega)\, e^{j\omega x_0} d\omega \tag{2.15}$$

By introducing in (2.15) the variable transformation $x_1=x+x_0/2$ and $x_2=x-x_0/2$, we obtain

$$f(x_1) f^*(x_2) = \frac{1}{2\pi} \int_{-\infty}^{\infty} W_f\left(\frac{x_1 + x_2}{2}, \omega\right) e^{j\omega(x_1 - x_2)} d\omega \tag{2.16}$$

and by substitution in Eq. (2.16) $x_1=x_2$ and $x_2=0$,

$$f(x)f^{*}(0) = \frac{1}{2\pi}\int_{-\infty}^{\infty} W_f(\frac{x}{2}, \omega)\, e^{j\omega x} d\omega \tag{2.17}$$

The Eq. (2.17) can be also interpreted as the necessary condition that a function of two variables must satisfy in order to be a WD. A more general study was be done by (de Groot 1972) that includes the necessary and sufficient conditions.

6. Product and convolution

The WD of a convolution of two signals f(·)and g(·) is equal to the convolution of the distributions in the spatial variable.

$$W_{fg}(x, \omega) = \int_{-\infty}^{\infty} W_f(x_0, \omega)\, W_g(x - x_0, \omega)\, dx_0 \tag{2.18}$$

The WD of a product of two signals f and g is equal to the convolution in the frequency variable.

$$W_{f \cdot g}(x, \omega) \int_{-\infty}^{\infty} W_f(x, \omega_0)\, W_g(x, \omega - \omega_0)\, d\omega_0 \tag{2.19}$$

7. Interference.

The WD computation of a multicomponent signal introduces spurious "cross- terms" due to its intrinsic bilinearity (Eq. 2.1). As recently has been pointed, the definition of a multicomponent signal is a controversial issue, because any signal can be split-up in an infinite number of different ways (Cohen 1989). The WD of the sum of two signals f(x)+g(x) is given by

$$W_{f+g}(x, \omega) = W_f(x, \omega) + W_g(x, \omega) + 2Re\,[W_{f,g}(x, \omega)] \tag{2.20}$$

where the last term in Eq. (2.18), that can be interpreted as the cross-WD corresponding to f(x) and g(x), is called "cross-term". The presence of cross-terms in the distribution, not necessarily are always undesirable. The recent work of Choi and Williams (Choi 1989) exploring particular members of the Cohen's class in order to minimize the cross-terms but retaining the basic

properties constitutes a major advance in the study of the time-frequency distributions.

C. Discrete Wigner Distribution

Although the WD was initially proposed for continuous variable functions, Claasen and Mecklenbräuker proposed at the beginning of the eighties a first definition for discrete variable functions (Claasen 1980b). However, one of the main disadvantages of the discrete definition is that not all the properties of the continues WD are preserved by discretization due to aliasing effects. In this sense several alternative definitions have been proposed in the literature in order to overcome this problem (Chan 1982), (Claasen 1983), (Brenner 1983), (Day 1983), (Peyrin 1986). It is shown that all the definitions are expressed by similar formulas and can be interpreted as a smoothed (filtered) version of the original elementary definition (Pacut 1989). The discrete WD of a sampled function f(n) is defined by

$$W_f(n,\omega) = 2\sum_{k=0}^{N-1} f(n+k)f^*(n-k)\,e^{-2j\omega k} \tag{2.21}$$

where n and $\omega=2\pi m/N$ are the spatial and frequency variables, respectively. The Eq. (2.21) can be interpreted as the N-point DFT of the image product

$$r_f(n,k) = f(n+k)f^*(n-k) \tag{2.22}$$

for a given point n.

The discrete WD is periodic in the frequency variable with period π, i.e. $W_f(n,\omega)=W_f(n,\omega+\pi)$. However, the signal's Fourier spectrum periodicity is 2π. The discrepancies between the different periodicity could be avoided by discharging the factor 2 in the exponent of the Eq. (2.21), but this has the drawback that the components in f at ω occurs at 2ω in the WD. This fact is a consequence of the intrinsic bilinearity of the definition given by the Eq.2.21 and produces that the simultaneous apparition of the even and odd samples occurs separately. This can result in aliasing unless analytic signals will be considered or by signal's oversampling by a factor of 2.

In the case of image applications, two problems arise in practice in order to compute the discrete WD. First, the aliasing problem can be reduced by smoothing the original image using low-pass filtering. One additional problem that appears in practice is the spectral dispersion or leakage due to the window size, specially important in the case of small sizes. To reduce leakage is necessary to introduce spatial apodization or truncation filters in order to minimize the spurious

side lobes of the sinc function, as a consequence of the windowing effect.

The discrete WD definition given by Eq. 2.21 retain the basic properties of the continuous WD, but introducing discrete-space signals. However, in that case the main difference comes from the inversion property. In the case of discrete signals, inserting k=n in Eq. 2.21 allows one to write

$$f(2n)f^*(0) = \sum_{m=-\frac{N}{2}}^{\frac{N}{2}-1} W_f(n,m)\, e^{-j2(\frac{2\pi m}{N})n} \tag{2.23}$$

From Eq. 2.23 only the even samples can be recovered. Inserting k-1=n in Eq.2.21 leads to the recovering of the odd samples

$$f(2n-1)f^*(1) = \sum_{m=-\frac{N}{2}}^{\frac{N}{2}-1} W_f(n,m)\, e^{-j2(\frac{2\pi m}{N})(n-1)} \tag{2.24}$$

In the case of image filtering operations the inversion property is crucial in order to manipulate the image in the Wigner domain and returning backwards to the spatial domain.

D. Wigner representation of images

The WD doubles the number of variables of the represented image. In this way, the WD of 2-D images is a 4-D function (2 spatial coordinates and 2 spatial-frequency coordinates). This fact is shown in the Figure 2.1, where a sinusoidal grating of 256x256 pixels, and with 4 period/image (Fig.2.1.a), as well as its WD (Fig 2.1.b) are displayed. Since the original image varies only in x direction, its WD is a 2-D function. This representation of the distribution is similar to the *information diagram* proposed by Gabor (Gabor 1946). The computation of this distribution involves a Fourier transformation for every point of the original image. These facts lead to consider the WD as a quite intensive process, that can limit the range of applications and image processing can be a good example of this situation. Different alternatives have been proposed in the literature in order to overcome these problems: optical processors, VLSI special purpose processors, and hybrid optical-electronic systems.

The most of the applications of the WD in image processing have been carried out through digital implementations (Jacobson 1982a, 1982b, Cristobal 1989, Gonzalo 1989, Gonzalo 1990b). This is a consequence of the characteristics of this kind of systems, such as the flexibility of being programmed, or the high speed and storage achieved for them in the last years.

From the definition of the discrete Wigner distribution function WD (see Eq.2.21) is clear that the first step to compute this distribution is to generate the corresponding *product function* $r_f(n,k) = f(n+k)f^*(n-k)$. Since here only real and positive value images will be considered, the function $f^*(\cdot)$ is equal to $f(\cdot)$; and then, the function $r_f(n,k)$ is obtained, for each value of k, by shifting k pixels the image represented in the spatial domain from the origin to left and to right, and multiplying these two images. For a particular test image, a composite rectangular grating with 32,16 and 8 pixels/period (Figure 2.2), its corresponding product function is shown in the Figure 2.3; each column represents a section of the product function associated with each value of k. The WD is obtained by computation the 1-D Fourier transformation of each column of the product function. The distribution of this composite grating is represented in the Figure 2.4. The frequency variable is mapped along the vertical axis, and the spatial coordinate along the horizontal axis.

Insert Fig. 2.2, 2.3, 2.4 about here

The figure 2.5 shows the WD corresponding to a rectangular window test. In this case, the distribution can be interpreted as a composite of $\text{sinc}(\cdot)=\sin(\cdot)/(\cdot)$ functions represented along the y-axis. Each one sinc's comes through DFT of the different image products corresponding to the different points selected in the spatial domain.

Insert Fig. 2.5 about here

The figure 2.6a shows an example of an aerial image with two main tree species, *Eucaliptus globulus* and *Pinus Pinea*. Figure 2.6.b shows on the top two samples of the image product, and on the bottom the corresponding samples of the WD.

Insert Fig. 2.6 about here

The WD constitutes an excellent framework in the study of local filtering operations. Cristobal *et al.* (1989) have carried out some digital space-variant filtering of images with one dimensional variation, and recovered the information of filtered image through the local spectrum power. The results of the operations after coming back to the original domain is shown in figure 2.7. The test image is shown in the Fig. 2.7a, and the local image power of the filtered image is displayed in Fig.2.7.b; a smoothing is obtained on the left hand side, and an edge sharpening on the right hand side, since the samples of the WD corresponding with the left half of the image were filtered with a low-pass filter, and the rest of the WD with a high-pass filter.

Insert Fig. 2.7 about here

E. Hybrid and digital implementations

The implementation and application of the Wigner distribution function is very appropriate to the characteristic of the hybrid processing. Since one of the main problems of this function is the throughout of computer time required, the most of the calculations can be performed via optical and to use the digital part to manipulate the information. The hybrid processors have a specific character, i.e., each problem required a different architecture; in fact, different architectures should be used to implement the same algorithm applied to different problems, this is the case of the WD (Easton 1984).

The idea of combining electronic technology with optical systems as a means to use the fast processing ability and parallelism of optics was proposed by Huang and Kasnitz (Huang 1967) and subsequently developed by Casasent et al (Casasent 1974). The WD computation can be done through the use of optical processors and storing the information in the computer for subsequent analysis.

Cristobal et al. (Cristobal 1989) presented a Wigner hybrid processor, based in the optical setup developed by Bamler (Bamler 1983) and shown in Fig. 2.8. Also in this case, the output of the optical system was 2-D spatial samples of the WD, associated with each point of the represented image. Then, this local spectrum were fed, via a TV camera, into a digital image processor, where the visualization and digital processing of this spectrum was possible. This hybrid processor has been recently improved by Gonzalo *et al.*(Gonzalo 1990a).

Insert Fig. 2.8 about here

Heretofore, the most applications of the time-frequency analysis in which the WD is computed correspond to the case of 1-D signals. As a result, Wigner analysis of speech, radar, sonar and biomedical signals become a reality. Real-time implementations for computing the WD of discrete signals have recently considered by the use of special purpose processors. In all the cases, the FFT plays a central role for the WD computation. Chester (Chester 1983) proposed a hybrid system in which a whole pre-processing: data acquisition, buffering, time reversal and windowing operations were done by a conventional serial computer DEC LSI-11, whereas the FFT was computed in special purpose hardware by using a dedicate microprocessor. The special symmetry properties of the discrete WD definition allow the computation of 2 WD's in one FFT cycle.

Boashash *et al.* (Boashash 1987) proposed the FFT computation by the use of a cascade of many processors connected in parallel. This method is effective for real-time applications, but increasing the system cost due to the large number of processors required. Sun *et al.* (Sun 1989) have recently reported an alternative system by using a pipeline implementation for the WD computation. The concept of pipeline processing besides in to divide the computational task in several sub-tasks, in such a way each sub-task is processed by a simple stage. Chester *et al.* (Chester 1989) have proposed more recently a hybrid system fully programmable capable of implementing discrete versions of the Cohen's class of functions, and in particular the WD. The implementation allows to capture wideband signals, by filtering and analytic baseband signal and decimating by a programmable rate. Once the baseband signal is generated, the WD is computed by using vector processors under the control of a RISC control processor.

In the case of images, the use of special purpose processors for time-frequency analysis have mainly been considered for the computation of the Gabor scheme of representation. Einziger (1986) proposed the use of VLSI modules for the computation of the elementary and/or auxiliary functions inherent in the Gabor scheme. Cristobal (1990) has recently proposed the use of cellular neural networks for the Gabor's receptive field computation. A machine vision based in the Gabor scheme should be implemented in special purpose VLSI hardware in order to take the advantages of the parallel architectures in computing the early vision processes, specially in the segmentation and feature extraction procedures. Hierarchical structures of computation retains the advantages of the local computations performed by the cellular automata, but simultaneously obtaining a capability for global computations. The pyramid structures may be considered as a combination of cellular arrays and tree structures (Tanimoto 1987). In the case of image processing applications, the main advantages of the pyramid schemes derive from the multi-resolution data representation. The pyramids have been considered as a general framework for implementing highly efficient structures of computation in which image compression, texture analysis and image motion are some illustrative examples of their use (Burt 1984). The pyramid structures are well suited for its implementations in VLSI circuits due to the fact one can be concentrated in a chip design that provides a "basic building array" of a reduced number of cells (i.e. 5x5 or 9x9 arrays). The whole architecture can be constructed by the interconnection of these basic structures (Tabernero 1990).

F. Cohen's unified approach and related distributions

It is interesting to introduce briefly some historical remarks about the origin and posterior advances of the joint time (space)-frequency distributions. Although this study is based on the

Wigner distribution, a more exhaustive discussion about the relations between the WD and other time-frequency distributions have already been considered elsewhere (Claasen 1980c), (Cohen 1989). Wigner was the first to have found, in the context of Quantum Mechanics, a function that simultaneously describe the position and momentum of a particle (Wigner 1932). In his first paper, he formulated that a bilinear distribution in the wave function ψ, satisfying the marginals (Eq. 2.9 and 2.10), cannot be always positive (the concept of a wave function ψ in Quantum Mechanics is formally identical to the concept of a signal f). This leads that the WD cannot be interpreted as a energy density function. However, this interpretation has minor significance in the image processing applications. When the positivity is a major requirement, different smoothed distributions has been proposed in the literature in order to obtain positive distributions, maintaining the rest of the properties. More details can be found in a recent paper by (Cohen 1989). Subsequently, Ville derived in the area of signal processing the distribution that Wigner proposed in Quantum Mechanics (Ville 1948). Many other authors use later also the Wigner-Ville or Ville distribution to denote the same distribution.

In the context of the time-frequency analysis it would be considered crucial the contribution of Dennis Gabor in his famous monograph "Theory of Communication" (Gabor 1946). The basic idea of the Gabor's theory implies the representation of a signal in terms of quanta of information named "elementary functions" or "logons", introducing the joint representation of signals by using the "diagram of information". He proved the principle that this kind of simultaneous representation is limited by the uncertainty relation. Following a proper formalism in Quantum Mechanics, Gabor derived by the use of the Schwarz inequality, which family of elementary signals minimizes the uncertainty relation between time and frequency. These elementary functions (now called Gabor functions) are gaussians modulated by sinusoids of the form

$$.f(x) = e^{-\frac{(x-x_0)^2}{\alpha^2}} e^{-j\omega x} \tag{2.25}$$

where ω represents the frequency of the sinusoid wave and x_0 and α represents the position and spread of the gaussian envelope.

The mathematical properties of these functions are discussed elsewhere (Baastians 1981). We will consider in Section IV the relevance of the Gabor's theory in the context of image applications.

Kirkwood in 1933 proposed another distribution, conceptually simpler than the WD given by

(Kirkwood 1933)

$$C(x,\omega) = \frac{1}{\sqrt{2\pi}} f(x)\, \mathcal{F}^*(\omega)\, e^{-j\omega x} \tag{2.26}$$

Rihaczek derived some time later the same distribution that he named complex energy spectrum giving some interesting insights about its physical interpretation (Rihaczek 1968). The Rihaczek distribution is related with the WD by a double convolution

$$C(x,\omega) = \frac{1}{2\pi} \int_{-\infty}^{\infty}\int_{-\infty}^{\infty} 2e^{-2j(\omega-\omega_0)(x-x_0)} W_f(x_0-\omega_0)\, dx_0 d\omega_0 \tag{2.27}$$

The distribution given by Eq. (2.26) is complex, but its real part is also a distribution that satisfies the marginals.

Page in 1952 proposed a new distribution named the instantaneous power spectra (see Table I), but the study was done by Mark (Mark 1970) by introducing the *physical spectrum*, which is basically the same concept of spectrogram, is worthwhile for its extensive use in different areas of research. The physical spectrum is related with the WD by

$$|S_w(x,\omega)|^2 = \frac{1}{2\pi} \int_{-\infty}^{\infty} W_w(x_0-x, \omega_0-\omega)\, W_f(x_0,\omega_0)\, dx_0 d\omega_0 \tag{2.28}$$

where w(x) represents a window function. The Mark's physical spectrum coincides with the square modulus of the complex spectrogram.

A general formulation of the bilinear time-frequency distributions was given by Cohen (Cohen 1966). Each member of the named Cohen's class is given by

$$C(x,\omega;\Phi) = \frac{1}{2\pi} \int_{-\infty}^{\infty}\int_{-\infty}^{\infty}\int_{-\infty}^{\infty} f(y+\frac{x_0}{2}) f^*(y-\frac{x_0}{2})\, \Phi(x,\omega)\, e^{-j(\omega x_0 - \omega_0 x + \omega_0 y)}\, dy dx_0 d\omega_0 \tag{2.29}$$

where the signal f(x) appears in the habitual bilinear form, and Φ is a so-called kernel function. The different members of the Cohen's class will be obtained as particular occurrences of the kernel Φ. For example, the WD and the ambiguity function can be obtained by taking $\Phi=1$ and $\Phi=\delta(x-x_0)\delta(\omega-\omega_0)$, respectively. This formulation has the advantage to give a general framework to a more systematic study of this time-frequency distributions. An interesting consequence of this formulation is based in the idea that placing constraints on the kernel one obtains a subset of

the distributions that have an particular property (Cohen 1966). Table I presents a summary of the main distributions and their corresponding kernels.

Table I. Some distributions and their kernels. Adapted with permission from (Cohen 1989)©1989 IEEE

Reference	Kernel Φ	Distribution $C(x,\omega)$
(Wigner 1932),(Ville 1948)	1	$\int_{-\infty}^{\infty} f(x_0+\frac{x}{2}) f^*(x_0-\frac{x}{2}) e^{-j\omega x_0} dx_0$
(Woodward 1953)	$\delta(x-x_0)\,\delta(\omega-\omega_0)$	$\int_{-\infty}^{\infty} f(x_0+\frac{x}{2}) f^*(x_0-\frac{x}{2}) e^{-j\omega x_0} dx_0$
(Margenau 1961)	$\cos\frac{1}{2}\omega x$	$Re\frac{1}{\sqrt{2\pi}} f(x)\, \mathcal{F}^*(\omega)\, e^{-j\omega x}$
(Kirkwood 1933)	$e^{\frac{j\omega x}{2}}$	$\frac{1}{\sqrt{2\pi}} f(x)\, \mathcal{F}^*(\omega)\, e^{-j\omega x}$
(Cohen 1966)	$\frac{\sin a\omega x}{a\omega x}$	$\frac{1}{4\pi a}\int_{-\infty}^{\infty}\frac{1}{x} e^{-j\omega x}\int_{(x-ax_0)}^{(x+ax_0)} f(x+\frac{x_0}{2}) f^*(x-\frac{x_0}{2})\, dx dx_0$
(Page 1952)	$e^{\frac{j\omega\lvert x\rvert}{2}}$	$\frac{\partial}{\partial x}\left\lvert\frac{1}{\sqrt{2\pi}}\int_{-\infty}^{x} f(x_0) e^{-j\omega x_0} dx_0\right\rvert^2$
(Mark 1970)	$\int_{-\infty}^{\infty} w(x+\frac{x_0}{2}) w^*(x-\frac{x_0}{2}) e^{-j\omega x} dx$	$\left\lvert\frac{1}{\sqrt{2\pi}}\int_{-\infty}^{\infty} f(x_0)\, w(x-x_0) e^{-j\omega x_0} dx_0\right\rvert^2$
(Choi 1989)	$e^{-\frac{\omega^2 x^2}{\sigma}}$	$\frac{1}{4\pi^{3/2}}\int_{-\infty}^{\infty}\int_{-\infty}^{\infty}\sqrt{\frac{\sigma}{x^2}} f(\xi+\frac{\xi_0}{2}) f^*(\xi-\frac{\xi_0}{2}) e^{-\frac{\sigma(\xi-x)^2}{4\xi_0^2}-j\omega x_0} d\xi d\xi_0$

We will discuss here a remarkable work published by Choi and Williams (Choi 1989) in the study of new distributions with desirable properties but simultaneously reducing the presence of undesirable effects. Some researchers have considered the WD as a *masterform* distribution from which the rest of distributions can be derived (Bartelt 1980), (Jacobson 1988), (Reed 1990). Choi

and Williams found that by an appropriate kernel selection, one can reduce the presence of cross-terms for multicomponent signals but retaining the rest of desirable properties (see Table I). The parameter σ in the kernel.

$$\Phi(\omega, x) = e^{-\frac{\omega^2 x^2}{\sigma}} \tag{2.30}$$

regulates the presence of cross terms. In the limit $\sigma \rightarrow \infty$ the Choi and Williams distribution becomes the WD. The presence of cross-terms is reduced for small values of σ, and the rate of cross-term decreasing is proportional to $1/(\sqrt{\sigma})$. Several different applications of the use of this new distribution has been reported in the study of speech, cortical event related potentials (ERPs) and electromyograms (EMGs) (Williams 1989). The importance of this work would be reflected in the different methodology to obtain distributions with desirable properties. Instead to modify the WD in order to reduce the cross-terms, one is interested to change the kernel for which the spurious values of the distribution are minimal. The definition of the Choi-Williams distribution kernel (Eq. 2.26) includes only a modifiable parameter σ, but the same method can be explored in the future to find new distributions with desirable properties.

The presence of cross-terms can be obscured the importance of the auto-terms specially for such applications in which the signal discrimination and recognition is a critical issue. For instance, in the analysis of speech signals the presence of these artifacts can be lead to a misunderstanding of the presence of formants. In the case of medical applications these artifacts can be difficult the signal analysis and hence the posterior diagnosis. Recently, Sun et al. (Sun 1989b) have proposed the elimination of the cross terms via pre-processing filtering based in the use of averaging or median filters. The basic idea is to consider the pseudo-Wigner distribution as an image with polarity eliminating the negative values by using classical convolution masks.

Another alternative to the reduction of the cross-terms is the use of the analytical signal rather than the real signal itself. This fact has the advantage to retain the original WD definition without introduce a smoothing factor in the kernel. Zhu et al. (1990) have reported recently the use of a 2-D Hilbert transform for Wigner analysis of 2-D real signals. They proposed a 2-D continuous Hilbert transform based in the Read and Treitel discrete Hilbert transform (Read 1973). The theoretical performance of the 2-D analytic signals in the WD computation was illustrated by Zhu et al. (1990) by using simulated and real images. However, the 2-D analytic signal, unlike the 1-D analytic case is not unique. Then, it is necessary to decide which 2-D analytic signal can be used in order to reduce various possible interference terms. In general, the appropriate choice of the 2-D analytic signal depends of the spectral signal characteristics. Recently, Zhao et al. (Zhao 1990) and Atlas et al. (Atlas 1990) have also proposed the use of a gaussian kernel in order to reduce the

interference terms but retaining the finite-time support and good frequency resolution.

Further research is needed both in the study of smoothing kernels and/or the 2-D analytic signals for image feature extraction and pattern recognition by using the WD spectral analysis.

III. Image Analysis through the Wigner Distribution

Texture is one of the attributes employed to characterize the surface of an object. However, there is not a unique definition of the notion of texture. Its definition has been formulated in terms of an enumeration of properties such as fine, coarse, etc. Conceptually, texture could be defined as the arrangement or spatial distribution of intensity variations in an image (Jernigan 1984). The two major characteristics of a texture are its coarseness and directionality. Since the spatial frequency domain representation contains explicit information about the spatial distribution of an image, one could expect to obtain useful textural features from the spatial frequency domain. However, the texture methods that embody spatial frequency information have met mediocre results (Sutton 1972), (Weszka 1976), mainly due to the fact that the Fourier transform is an intrinsically global transformation, i.e. each frequency component contains global information about the whole image. Even reducing the window size to contain homogeneous texture sub-images was not an advantage in comparison with the spatial methods based in the use of second-order probabilities (co-ocurrence methods).

Here we have considered the use of the space-frequency representations, namely the WD, in the case of image analysis applications. A recent review about the use of the joint representations mainly in the areas of signal and speech processing can be found in (Cohen 1989). In Section VI a summary of these applications is presented, considering also the use of these representations in the image and vision modeling research.

Recent studies have suggested that the visual texture discrimination ability is achieved locally (Gagalowitz 1981), (Julesz 1983). The WD entails a rigorous framework in the use of local representations, in such a way it embodies the spectral local variations that can improve the texture discrimination and segmentation processes. In this way, we have considered the use of the WD for texture discrimination and classification, in the statistical approach.

Texture features can be described by generalized filtering techniques through image transforms. Fourier spectral analysis has been applied for discrimination of terrain types (Lendaris 1977) and for detection and classification of lung diseases by comparing the normal and abnormal textural features (Kruger 1974). In the present study, the WD based method for texture classification has been applied to four Brodatz texture field examples (Brodatz 1966). A complete archive of digitized images, including the Brodatz textures, can be found in (Weber 1989). Figure 5.2a represents the four textures selected (clockwise from top left) sand, straw, raffia and cotton canvas. The texture samples were digitized and converted into 256x256 picture arrays with 8 bit/pixel from (Brodatz 1966). One of the advantages in the use of the WD is that the window size

selection is not required. However, in order to reduce the computational requirements it's necessary to relax the definition and to define a specific window size. Different window sizes have been proposed in the literature to obtain a good statistical resolution (Ashjari 1980), (Pratt 1980). Here we have used N=16 texture fields of 64x64 pixel each.

A. Feature extraction

The first order statistics of all textures have been normalized to uniform distributions using histogram equalization, so that differences in luminance and contrast are eliminated in the discrimination process. The histogram of an image represents the frequency of ocurrence of the gray levels along the image. By histogram equalization we can obtain an output image in which the gray levels of the picture are more uniformly distributed than in the original image. Figure 3.1 shows an example of the resulting histogram equalization of the intensity mapped image

.

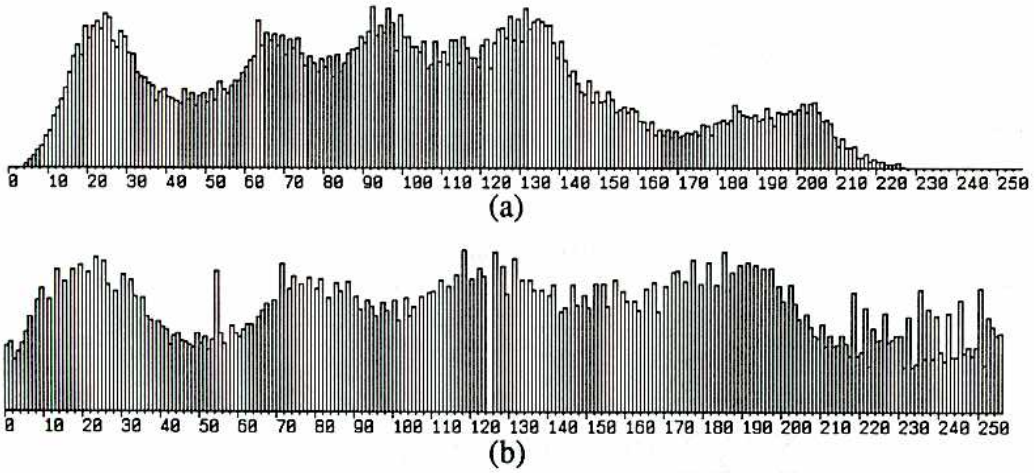

Figure 3.1. (a) Original Girl (Lenna) histogram. (b) Equalized histogram corresponding to Fig.3.1a

The histogram-modeling techniques has been considered as a powerful approach to the image enhancement applications. An example of the utility of these techniques is the case of images with narrow histograms (low-contrast images). By histogram equalization one can increase the image contrast as a consequence of the histogram stretching (Gonzalez 87), (Jain 89). After performing histogram equalization on textures, a complete homogeneity of the data is reached, and any result from the computation is solely due to the intrinsic texture structure and not to undesired luminance biases. Figure 3.2a shows the four preprocessed Brodatz textures selected in the forthcoming study (Brodatz 66). Figure 3.2b shows the corresponding Fourier spectra.

Insert Fig. 3.2 about here

The evaluation of the WD's categorization capabilities requires the election of the most discriminant features. The method proposed here is based in the computation of the auto-WD at N=16 different points of the texture separated by 2 pixels, and the corresponding selection of features from such distributions to obtain the texture feature vector. The auto-WD was sampled in I=16 annular regions and H=8 angular sectors, using a similar sampling scheme to the Fourier power spectrum methods (Stark 1982). The features extracted from the WD were the following (Cristobal 1989)

$$w_1 = \frac{\sum_{i=1}^{I} \left[\sum_l \sum_m \rho W_f^2(l,m) \right]_{\forall (l,m)\, inringi}}{\sum_l \sum_m W_f^2(l,m)} \tag{3.1}$$

$$w_2 = \frac{\sum_{i=1}^{I} \left[\sum_l \sum_m (\rho - w_1)^2 W_f^2(l,m) \right]_{\forall (l,m)\, inringi}}{\sum_l \sum_m W_f^2(l,m)} \tag{3.2}$$

$$w_3 = \frac{\sum_{h=1}^{H} \left[\sum_l \sum_m \theta W_f^2(l,m) \right]_{\forall (l,m)\, insectorh}}{\sum_l \sum_m W_f^2(l,m)} \tag{3.3}$$

$$w_4 = \frac{\sum_{i=1}^{I} \left[\sum_l \sum_m (\theta - w_3)^2 W_f^2(l,m) \right]_{\forall (l,m)\, insectorh}}{\sum_l \sum_m W_f^2(l,m)} \tag{3.4}$$

$$w_5 = \frac{1}{\left| W_n^2(0,0) - W^2(0,0) \right|} \tag{3.5}$$

where $\mathbf{W^2(0,0)}$ is the mean value of the WD at the N selected points, and ρ, θ are the polar coordinates in each local WD spectrum. The physical interpretation of the proposed features is as follows. The feature w_1 gives a measure of the mean spatial frequency content of the image. It will have low values for images with a limited grade of detail and increasing in the case of sharpness images. The feature w_2 is a variance estimation of the feature w_1 and gives a measure

of the contrast or the amount of the luminance local variations of the image. The feature w_3 and w_4 give a measure of the mean directionality and its variance, respectively. The feature w_5 is a measure of the homogeneity of the image. This measure is based in one of the properties of the Fourier transformation: the value at the origin represents the mean value of the original image (Bracewell 86). These features has been arranged as a 5-D pattern vector w which constitutes the input to the classification process (see Fig. 3.3).

Insert Fig. 3.3 about here

The same procedure has been applied for comparison purposes to the same data texture tests by the computation of the Fourier transformation directly to the windowed images. The results are illustrated in the next section.

B. Classification

The evaluation of the statistical texture measures can be done by using direct methods through classification errors or by indirect methods which involves classification errors estimation via the use of a figure of merit. In this study, the texture features proposed in Section A have been evaluated with other methods according to their Bhattacharyya distance (B-distance). The B-distance is a scalar function of the probability densities of the features of two classes, and is given by

$$B(S_1, S_2) = -ln\{\int [p(x|S_1)\, p(x|S_2)]^{1/2} dx\} \tag{3.7}$$

where **x** and $p(x|S_i)$ represent a feature vector and the conditional density probability for class S_i. In the case of bayesian classifiers the B-distance is monotonically related with the Chernoff bound of the probability of classification error. This lower bound is given by (Fukunaga 1972),

$$P_e \leq [P(S_1)\, P(S_2)]^{1/2} e^{-B(S_1, S_2)} \tag{3.8}$$

where $P(S_i)$ represents the *a priori* probability associated to the class i. For Gaussian probability densities, the B-distance between a pair of texture classes is given by,

$$B(S_1, S_2) = \frac{1}{8}(m_1 - m_2)\left[\frac{\Sigma_1 - \Sigma_2}{2}\right]^{-1}(m_1 - m_2)^T + \frac{1}{2} ln\left[\frac{|(1/2)\,(\Sigma_1 + \Sigma_2)|}{|\Sigma_1|^{1/2}|\Sigma_2|^{1/2}}\right] \tag{3.9}$$

$\mathbf{m}_i$ and Σ_i represent the feature mean vector and feature covariance matrix of the class i (Fukunaga 1972). For equally likely texture field pairs, i.e. $P(S_i)=P(S_j)$, a B-distance of 4 or greater corresponds to a classification error of about 1% (see Table II)

Table II. B-distance versus the error probability, according to Eq. 3.7

$B(S_i, S_j)$	Error bound ($x10^{-3}$)
1	184
2	67.6
3	24.9
4	9.16
5	3.37
6	1.23

The selection of the image windowing process was done as follows. Figure 3.4a shows sixteen product images corresponding to the cotton canvas texture image at points (128,48), (128,50),...,(128,80) and Figure 3.5a shows the corresponding product images for the straw texture at these points. The associated Fourier transform at each point, i.e. its WD, is displayed in Figures 3.4b and 3.5b respectively, that show the effects of the object periodicity and directionality. Similar results would be obtained in the case of the sand and raffia textures.

Insert Fig. 3.4, 3.5 about here

The texture feature extraction method here is based on the features previously proposed in Eq. 3.1-3.5. The ability to discriminate texture pairs using the WD features was compared with the classic Fourier's spectral energy method. In the Fourier method, the sampling scheme used was the summation within five concentric rings centered in each 64x64 spectrum, giving the feature vector $\mathbf{f}=[f_1,f_2,f_3,f_4,f_5]^T$. The results of the pairwise B-distance computation have been tabulated in Table III.

Table III. Textural B-distance in the Fourier and Wigner Feature Extraction Methods.

Texture pair	Fourier Method	Wigner Method
Sand-straw	0.9	104.74
Sand-cotton	1.86	48.44
Sand-raffia	0.99	4.84
Straw-raffia	2.18	24.31
Straw-cotton	0.76	71.92
Cotton-raffia	2.59	34.17
Mean pair	1.55	48.07

In the Fourier method the sand-straw pair is the most similar, i.e. the error probability is the biggest, and the cotton-raffia is the least similar. In contrast, in the WD method the sand-raffia pair is the most similar and the sand-straw pair the least similar. From Table IV one can argue the WD discrimination of natural textures (generally random) outperforms the Fourier methods. In contrast, the artificial textures (often periodic and deterministic) are well discriminated by the Fourier methods as one can expect due to its intrinsic harmonic expansion. The B-distance has been computed using a conventional statistical package (IMSL 1982).

In addition to the pairwise linear discrimination, we have considered multiple discriminant analysis in order to obtain the 2-D subspace which maximizes the ratio of between class scatter to within class scatter (Fisher's discriminant) (Duda 1973). If $\mathbf{w}$ is the direction which defines the linear discriminant plane, the Fisher ratio is given by,

$$J(w) = \frac{|m_1 - m_2|^2}{\sigma_1^2 + \sigma_2^2} \tag{3.9}$$

where m_1 and m_2 correspond to the mean projections along the discriminant direction defined by $\mathbf{w}$, i.e. $m_i=\mathbf{m}^T\mathbf{w}$; $\mathbf{m}$ represents the mean vector associated to each class, and ${\sigma_1}^2$ and ${\sigma_2}^2$ the summed squared difference between the projected classes and the mean class, i.e.

$$\sigma_i^2 = \sum_{x \in \omega_i} |w^T (x - m)|^2 \tag{3.10}$$

Projections of the samples from the 5-D space to this plane give a scatter diagram of the texture classes, which is a suitable class's discriminant representation. Figure 3.6a shows the best scattered plane for the Fourier feature extraction method, and Figures 3.6b and 3.6c show the corresponding scattered diagram for the co-ocurrence method and WD method, respectively (the scales have been adjusted to aid the comparison). In these plots we can observe a higher interclass discrimination in the WD method in comparison with the other methods used; in contrast, the clusters are less compact (worse intra-class discrimination) than the Fourier or co-ocurrence methods. The co-ocurrence methods are based on the estimation of the second-order joint conditional probability density functions $p(i,j \mid d,\theta)$, where each p represents the joint probability from gray level i and j, given the intersample distance d and orientation θ. The estimated values can be written in a matrix form, that constitutes a second order histogram. From this histogram several textural features can be extracted. Conners and Harlow have proposed the use of five descriptors extracted from the co-ocurrence matrices: energy, inertia, entropy, correlation and local homogeneity (Conners 1980), originally proposed by Haralick (Haralick 1979). For a discussion about the texture analysis methods see (Van Gool 1985).[1]

Figure 3.6 about here

C. Texture Discrimination

In this Section we will consider the WD's texture discrimination abilities. Image description requires segmenting it into regions which are homogeneously textured. One of the most commonly methodologies to image segmentation involves edge detection processes where a transition occurs from one uniform region to another. An alternative approach to segmentation is region growing, starting from small uniform regions, and expanding the process until the uniformity is broken.

The segmentation processes can be evaluated by the use of texture pairs. The significance of texture pairs comes from the fact that any texture analysis problem can be split in an equivalent texture pair (Davis 1981). A simple 1-D texture discrimination mechanism is proposed based in the use of the WD. The pixel categorization of the texture pixels was formulated by (Davis 1981) in terms of edge pixel, near-edge pixel and interior pixel. Here, the texture edge detection is based

1. A complete bibliography about vision is yearly published by A. Rosenfeld in the journal Computer Vision, Graphics and Image Processing (Academic Press). An on-line version is located at host ads.com and can be accesed via ftp at directory pub/VISION-LIST-ARCHIVE/ROSENFELD-BIBLIOGRAPHIES

on the computation of differences between the WD in adjacent points along a selected direction and the WD mean. Figure 3.7a shows a texture pair (cotton canvas-raffia) and Figure 3.7b shows from left to right and top to bottom the WD at the 16 points selected along the x-axis. The window size was 64x64 pixels in order to obtain a good statistical resolution. The evaluation of the edge detection was realized by introducing the scalar parameter e_W for a given point (i_0,j_0). It is given by

$$e_W(i_0,j_0) = \sum_{i=1}^{k}\sum_{j=1}^{k} \left| W_n(i,j) - \overline{W}(i,j) \right| \tag{3.11}$$

where $\overline{W}$ is the WD mean associated to the N points selected,

$$\overline{W}(i,j) = \frac{1}{N}\sum_{n=1}^{N} W_n(i,j) \tag{3.12}$$

Insert Fig. 3.7 about here

Figure 3.8(a-d) shows the plots of e_W versus d (interpixel distance) for four texture pairs. A pronounced minimum can be observed in the four examples, denoting the presence of a textural border. This fact permits to conclude that the WD method might be give a good discriminability in the case of edge pixels and near edge pixels.

Insert Fig. 3.8 about here

Jau and Chin (Jau 1988) have proposed the use of the change in texture density (texture gradient) as an estimator of surface shape. The method is based by measuring the high frequency WD local contribution at each location of the image. From this measures, a map description can be used to estimate the surface orientation. The method was implemented in the case of planar surfaces. Recently, Reed and Wechsler (Reed 1990) have proposed the use of a relaxation method for the boundary edge detection in the case of synthetic textures and Brodatz textures. The region labeling was performed by a double process of averaging and squashing transformation. Afterwards, they have presented the segmentation results in the case of synthetic textures different in phase only (identical power spectra) showing that due to the fact the WD encodes the magnitude and phase information, the formulation of features to take account the phase is not required. Finally, they have applied the relaxation mechanism to the Gestalt (proximity) clustering. However, the results reported on the use of the WD for image segmentation require

further study and extension to a large image database.

Related works on the use of space-frequency distributions for image segmentation purposes have been reported in the literature. Mostly of them are related with the use of the Gabor representation. Porat and Zeevi (Porat 1989) have proposed a texture feature extraction and segmentation based in the use of Gabor expansion coefficients. Perry and Lowe (Perry 1989) have proposed the use of an iterative edge segmentation mechanism by local Gabor filters. Malik and Perona (Malik 1989) have considered the use of radial and directional gaussian derivatives filters in the fitting of the receptive field data according to the Young's model (Young 1985). They applied the model for texture boundary detection in the case of natural and artificial scenes, and evaluated the degree of discriminability for different textured pairs used in psychophysical experiments.

On the other hand, a computational approach for analyzing textures based in multiresolution schemes of representation (also known as multichannel or pyramidal schemes) through the use of space-frequency distributions have been recently considered. Bovik et al. (Bovik 1990) have proposed a multichannel scheme of representation, based in Gabor filters, by encoding the images using multiple narrow band-pass and orientation channels. By comparing the magnitude of the response of different channels, textural border information can be extracted. The scheme was applied in the case of natural and synthetic textures for segmentation purposes. Tan and Constantinides (Tan 1990) have proposed a similar multichannel system based in the use of Gabor filters for texture segmentation for natural and artificial textures, reporting very satisfactory segmentation results.

The importance of the local phase in the feature detection and texture segmentation has been considered recently in different works. It is well known that the symmetry of edges and lines is reflected in the phase spectrum. Concetta and Burr (Concetta 1988) have proposed a biological plausible model of feature detection based in the use of the local phase through filters in quadrature and reporting some remarkable experiments on the prediction of the position of perceived features. Zeevi and Porat (Zeevi 1988) and Behar et al. (Behar 1988) have reported the use of the localized phase by using Gabor filtering for image reconstruction. Finally, Bovik et al. (Bovik 1990), in the same work already referred, have considered the use of the local phase for image segmentation. The use of the localized phase is specially useful to detect boundaries between textures having identical amplitude spectra. A pair of mirrored images constitute a good example of this situation. In these cases the amplitude-based methods fails to discriminate between the different regions with the same amplitude spectra.

IV. Applications of the space (time)-frequency representations

A. Review of applications

In this Section we will consider the different areas of research in which the space (time)-frequency representations have been applied. Obviously, the use of this kind of representations is quite appropriate for every field where nonstationary signals appear. As Cohen has pointed in a recent review (Cohen 1989), the applications can be broadly categorized according to two basic ideas: the extraction of relevant information from the distribution, or the use of a particular property which clearly represents the space (time)-frequency contents. Table IV presents an update survey about the application areas in which the use of these representations have been considered. The classification has been done according with the main topics of interest in which the distributions have been applied: signal, speech and vision. The vision and speech applications are separately considered from the rest of applications due their importance in the study of perceptual signals. Here, the vision applications have been emphasized, and the next section is concerned with the importance of these distributions in the modeling of the visual early processes.

In relation with the signal processing applications (see Table IV), perhaps the two main domains considered up to now would be the seismic signal exploration and the biological signal processing. Boashash was the first to use features extracted from the Wigner Distribution in the computation of the dispersion and attenuation of seismic signals (Boashash 1978). In the case of biological signal processing, these distributions have been applied in the analysis and design of ultrasonic transducers (Marinovic 1986) for medical imaging purposes. The time-frequency representations constitutes an excellent aid to the transducer design by means of which the desired response can be modified and visualized.

One of the main difficulties on the analysis of the speech signals derives from its intrinsically nonstationary character, i.e. the signal's frequency content varies with the time. This fact justifies the considerable interest in the use of time-frequency representations specially in the earlier stages of speech processing. From the pioneering work of Gabor, on the use of joint representations in the analysis or hearing (Gabor 1946), different speech applications have been considered in the literature. Table IV summarizes the applications reported in the area of speech applications.

Recently, the interest for the use of space-frequency representations has been extended to the vision research through the use of the Wigner Distribution (Jacobson 1982a, 1982b, 1984), (Cristobal 1986, 1987,1989), (Gonzalo 1989, 1990a), (Zhu 1990). The WD gives an image joint

representation suitable for the study of the non-stationarities such as spatial-variant degradations: progressive blurring, motion, texture, etc. Therefore, the WD entails a powerful framework for image analysis due to its intrinsic local nature (see Table IV). In a recent study, Jacobson and Wechsler have concluded that the resolution (uncertainty) attained by the WD cannot improved by some other different joint representations derived from the Cohen's class, as a consequence of the smoothing effect derived from the kernel's election (Jacobson 1988). However, a considerable number of works have been reported on the application of the Gabor transform in image applications, some of them have been summarized in Table IV. Perhaps, the principal reason for this interest is due to the fact the Gabor scheme of representation is biologically plausible, and hence able to serve as a suitable vision model at the retinal ganglion cells, the lateral geniculate nucleus and the primary cortex (De Valois 1988), (Van Essen 1990). The same argument can be applied in the case of speech signals, in which some neurophysiological (Kay 1972) and psychophysical (Møller 1978) studies have demonstrated that a large population of the auditory cells in the mammalian cochlear nucleus do not respond optimally to continuous tones, but instead responding to different preferred modulation slopes (directional selectivity).

Table IV. Survey of time(space)-frequency applications

Area I: Signal Processing

Subarea	Comments	Sources
Seismic exploration	Absorption and dispersion measurements by the WD	(Boashash 1978),
id.		(Bazelaire 1987)
Pattern Recognition	Classification of linear FM signals by the WD	(Kumar 1983)
Loudspeaker design	Extraction of optimization criteria by the WD	(Janse 1983)
Turbulence microstructure	Analysis of temperature gradient records by WD	(Imberger 1986)
Ultrasonic transducers		(Marinovic 1986)
Machine noise	Signaturing, detection and identification by WD	(Boashash 1988)
Muscle sounds	Signal analysis by using the Choi-Williams distribution	(Choi 1989)
Temporomandibular sounds	WD-based non-invasive diagnosis technique	(Zheng 1989)
Radar imaging		(Boashash 1989)
ECG analysis	Detection of P-waves by the WD	(Abeysekera 1989)
	Body surface potential mapping series of ECG's	(Usui 1990)
Sonar	Use of cone-kernel for range-doppler estimation by WD	(Atlas 1990)

Area II: Speech Processing

Subarea	Comments	Sources
Speech discrimination	Analysis of hearing by joint representations	(Gabor 1946)
Study combined representations		(Preis 1982)
Speech recognition		(Chester 1983)
id.	Time-delay representations	(Waibel 1989)
id.	Time-varying filtering by short time Fourier transform	(Asi 1990)
Survey bilinear representations	Analysis of hearing by joint representations	(Szu 1987)
Speech and musical analysis	Formant's visualization by wavelet transforms	(Kronland 1987)
Formants structure	Speech formant segmentation by the WD	(Riley 1987,1989),
id.	Analysis consonant-vowel transitions	(Velez 1989)
id.	Cone-kernel definition to reduce cross-terms by the WD	(Atlas 1990)
		(Zhao 1990)

Area III: Vision Processing

Subarea	Comments	Sources
Conformal mapping	Invariant pattern recognition through the WD	(Jacobson 1982a,b, 1984)
Image analysis	Texture classification and discrimination through the WD	(Cristobal 1986, 1987,1989)
id.	Analysis of local spectra by using analytic signals	(Zhu 1990a, 1990b)
Speckle Imaging	Discrimination using Gabor filters	(Paler 1986)
Optical flow	Spatiotemporal velocity analysis through the WD	(Jacobson 1987)
id	Spatiotemporal motion-energy Gabor filters	(Heeger 1987)
Image restoration	Spatial-variant filtering using the WD	(Berriel 1988),
id.		(Gonzalo 1988, 1990)
Texture analysis and clustering	Segmentation through the WD	(Reed 1988, 1990),
id.	Feature extraction using Gabor filtering	(Porat 1989)
id.	Segmentation by Gabor and wavelet filtering	(Perry 1989)
Shape from texture	Surface orientation by texture gradient using WD	(Jau 1988)
Stereo	Local disparity information by Gabor filtering	(Jenkin 1988),
id.		(Sanger 1988)
Motion	Spatio-temporal energy filtering using Gabor filters	(Adelson 1985)
Image compression	Gabor filtering encoding by neural network relaxation	(Daugman 1988)
id	Multiresolution techniques by wavelet filtering	(Mallat 1989)
Face recognition	Graph matching by Gabor filtering	(Buhmann 1989)

By the time this review will be appear, a monograph on recent time-frequency applications will be edited by (Boashash 1990).

B. Trends towards biological image modeling.

One of the actual trends in the vision research is concerned with learning as much as possible from the biological visual systems, for its implementation in artificial systems. From the pioneering experimental work on neurons of Hubel and Wiesel in the visual cortex (Hubel 1962), different biological-based models have been considered in the literature (Marcelja 1980); (Daugman 1980); (Young 1985). In most of them, the main interest is centered on the specification of the basic primitives of the early vision which can be inferred from the experimental biological recordings. The receptive field profiles in the retina and the visual cortex can be approximated by Gabor functions. However, it is necessary to remark which alternate mathematical descriptions of receptive fields are possible, with equal or even better results, as far the physiological data modeling concerns (Young 1885), (Koenderink 1990). The Gabor approach is related with the representation of time-varying signals in terms of elementary functions ("logons") that are simultaneously localized in time and frequency. Following a Quantum Mechanics's formalism, Gabor proved, by the use of the Schwarz inequality, the family of functions that achieve the lower bound of uncertainty in the joint time-frequency domains. In the frequency domain, the Gabor functions constitute a family of band-pass filters which captures the most salient properties of spatial frequency and orientation selectivity. The compactness of Gabor functions in the frequency domain also implies that the Gabor's original scheme should be nearly locally complete (i.e., close to encode all the input information with negligible aliasing) (Geisler 1986).

The Gabor scheme of representation is defined by a filtering process based in the use of complex-valued weighting functions given by:

$$h(x,y) = f(x,y) + jg(x,y) = f(x,y) - j\hat{F}(x,y) \tag{4.1}$$

where f(·), g(·) are real valued functions, and $\hat{F}(x,y)$ represents the Hilbert transform of f(·). In signal analysis and optics, the complex function h(·) is known as the analytic signal associated to f(·). The Hilbert transform g(·) is referred as the quadrature function of f(·). This scheme of complex filtering can be implemented in a real visual system by a pair of receptive fields in quadrature. The family of Gabor filters is given by gaussians tapered by sinusoids

$$f(x,y) = e^{-\pi\left[\left(\frac{x-x_0}{\sigma_x}\right)^2+\left(\frac{y-y_0}{\sigma_y}\right)^2\right]}\cos\{2\pi(u_0(x-x_0)+v_0(y-y_0))\} \tag{4.2}$$

$$g(x,y) = e^{-\pi\left[\left(\frac{x-x_0}{\sigma_x}\right)^2+\left(\frac{y-y_0}{\sigma_y}\right)^2\right]} \sin\{2\pi(u_0(x-x_0)+v_0(y-y_0))\} \quad (4.3)$$

where σ_x and σ_y represent the gaussian spreads at 1/e along the x-axis and y-axis respectively. The parameters u_0 and v_0 represent the tapering sinusoidal modulation envelope which define the frequency magnitude: $f_0 = \sqrt{u_0^2+v_0^2}$ according with the direction $\theta_0 = tg^{-1}(v_0/u_0)$. If a circularly symmetric condition is imposed ($\sigma=\sigma_x=\sigma_y$), the Gabor filter is uniquely defined by three parameters σ, f_0 and θ_0. The Fourier transform of the complex filter $\mathcal{H}(u,v)$ defined by Eq. 4.1 is

$$\mathcal{H}(u,v) = \frac{[\mathcal{F}(u,v) + \mathrm{sgn}(u)\,\mathcal{F}(u,v)]}{2} \quad (4.4)$$

for a given v, where $\mathcal{F}(u,v)$ represents the Fourier transform associated to f(x,y). From Eq. 4.4, it is obvious to see that positive spatial frequencies $\mathcal{H}(\cdot)$ is identical to $\mathcal{F}(\cdot)$ and for negative frequencies is equal to 0. This means that the complex filter h(·) transmits the same information that its real part f(·). Similar relations could be obtained in Eq. 4.4 by using the function sgn(v). If f(·) is a Gabor filter (gaussian tapered by a sinusoid) then g(·) is given by the quadrature filter (gaussian modulated by a co-sinusoid). Figure 4.1 shows a pair of Gabor filters in quadrature in the case of 1-D signals.

Insert Fig. 4.1 about here

Figure 4.2 represent in a 3-D space a parametric plot of the analytic filter associated to the same quadrature filters defined in Figure 4.1.

Insert Fig.4.2 about here

Once the parameters of the filtering process have been defined, the extraction of the local energy and local phase can be done by

$$e(x,y) = i(x,y) \otimes f(x,y) \quad (4.5)$$

$$o(x,y) = i(x,y) \otimes g(x,y) \quad (4.6)$$

$$\mathcal{E}(x,y) = \sqrt{e(x,y)^2 + o(x,y)^2} \quad (4.7)$$

$$\phi(x,y) = tg^{-1} \cdot \left[\frac{o(x,y)}{e(x,y)}\right] \quad (4.8)$$

where i(·) represents the input image and f(·) and g(·) are the filters in quadrature. Eq. 4.7 gives the amplitude of the analytic signal and provides an information about the local energy that is independent of the phase. This operation embodies a half-wave rectification mechanism. The rectification process has a biological foundation in the fact that neurons can give only non-negative response. A mechanism that compute the square-outputs of a quadrature pair of filters is known as an energy-mechanism. The importance of the remaining information encoded in the phase (Eq. 4.8) has been pointed by (Zeevi 1988). In the cited work, they demonstrated that the local phase-mechanism preserved most of the edge information contents of an image (in a similar manner to the Fourier phase-analysis).

In this section, we summarize some experimental results in order to have a quantitative measure of the degree of biological plausibility. In the physiological experiments the recordings are generally reported from cat and monkey retinal ganglion cells, lateral geniculate cells and cortical cells (area 17, layer IV) due to the high degree of similitude with the human visual system.

As already was mentioned, Hubel and Wiesel (Hubel 1962) studying the cat's visual cortex, reported that most cortical cells have orientation and frequency selectivity. From a qualitative approach, they described the receptive field response of the cortical simple cells as a composition of excitatory and inhibitory response. De Valois has recently reported that the bandwidth of the macaque cortical cells range from 0.5 and 8 octaves, being the median spatial frequency bandwidth of about 1.4 octaves (de Valois 1988). Quantitative measures of the receptive fields have been recently obtained by (Movshon 1978), (Webster 1985), (Field 1986), (Jones 1987), (Hawken 1987), (Emerson 1987), (de Valois 1988).

Next, we will give a short historical perspective about the receptive field's modeling. Mach in 1868 was the first to suggest that retinal interactions can be described in terms or second differential operators (laplacian operators) (Ratliff 1965). Kovasznay and Joseph were the first to apply the laplacian operator to image processing (Kovasznay 1953). Marr and Hildred have proposed the use of the laplacian of a gaussian for the early visual edge detection, showing that the simple difference of gaussians (mexican hat filters) can be approximate to the cat ganglion cell receptive fields (Marr 1980). Marcelja and Daugman have proposed the use of Gabor filters for 1-D and 2-D signals respectively (Marcelja 1980), (Daugman 1980). One alternative to the use of Gabor functions is the use of directional gaussian derivatives proposed by (Young 1985). The receptive field description is basically the same in both models, being the location of the zero-crossings the main difference. The similarities between both models are not surprising because in

the limit the two theories become the same. More recently, Canny has proposed an edge detection method based on the use of directional derivative gaussian functions (Canny 1986).

Another important characteristic is related with the receptive field symmetry. Hubel and Wiesel also reported the presence of even-symmetric and odd-symmetric cells, responding optimally in phase quadrature (Hubel 1962). Pollen and Ronner have obtained some recordings in the cat striate cortex from two adjacent simple cells, and found one member of the pair to be even-symmetric and the other to be odd-symmetric (Pollen 1981). More recently, Field and Tolhurst have found that pairs of adjacent cells differ by $\pi/2$ but appearing in a variety of different forms (not necessarily into even- and odd- symmetric categories) (Field 1986). A more detailed psychophysical study concerning the importance of the phase can be found in (Concetta 1988).

The experimental works reported here lead to conclude that the Gabor scheme or the gaussian derivative model not necessarily provide the best possible fit to all the recordings registered. In fact, some other mathematical functions can be tested. Young tested many other mathematical functions (Bessel, sinc, parabolic cylinder, etc.), and he found that the gaussian derivative as well as the Gabor functions provided the best fits to the recordings registered (Young 1985). However, one can say the main advantages of the Gabor/gaussian derivative models come from their effectiveness in providing a good fitting of the receptive field shapes with a limited number of free parameters (three in the case of the Gabor models). Signal expansions based in the use of Hermite polynomials has been recently considered as an alternative to the receptive field modeling which leads to a basic Gaussian derivative scheme (Martens 1990a). The Hermite polynomials proceed from the Quantum Mechanics wave functions corresponding to an harmonic oscillator. In this polynomial expansion Gaussian windowing functions are considered as well as a square sampling lattice. One of the advantages of this approach is the reduced number of free parameters: the Gaussian spread σ and the sampling distance T. Applications in hierarchical image coding and pattern classification have been recently reported by (Martens 1990b).

Mallat has recently pointed the use of the Gabor transform in computer vision presents several drawbacks when applied to image analysis (Mallat 1989a), (Mallat 1989b). The main difficulty comes from the constant resolution in the spatial and spatial frequency domains. This fixed resolution introduces some troubles specially if the image have important features of very different sizes. In other words, it is difficult to analyze simultaneously both the fine and coarse structures. In order to overcome these inconveniences, Grossmann and Morlet defined a decomposition scheme based on expansions in terms of translations and dilations of a unique function named 'wavelet' $\psi(x)$ (Grossmann 1984). The wavelet transform of a function $f(\cdot)$ is

given by

$$\Psi_f(a,b) = \frac{1}{\sqrt{|a|}} \int_{-\infty}^{\infty} f(x)\, \psi\left(\frac{x-b}{a}\right) dx \tag{4.9}$$

where $\psi(\cdot)$ is the basic wavelet. The parameters a and b can be chosen to vary continuously or discretely. The wavelet transform and the Gabor transform have many features in common. Both transforms analyze the frequency content of a signal locally in space. But the wavelet transform provides different resolutions for high versus low frequency wavelets, i.e. the basic functions $\psi(\cdot)$ have variable width and they are adapted to their frequency range: the higher was the range, the more narrow they are (Daubechies 1989). The different wavelet functions can be generated from a basic one through the following expression: $\psi_{mn}(x) = a_0^{-m/2}\psi(a_0^{-m}x - nb_0)$, where a_0 and b_0 are constants and m and n define the position and size of the new function. Some particular examples of wavelets have been obtained through the previous equation (Fig. 4.3).

Insert Fig. 4.3 about here

By using a multiresolution representation, Mallat has applied the wavelet transform to image compression, texture discrimination and fractal analysis (Mallat 1989a). This kind of representation is specially well suited for evaluating the self-similarity of a signal and its fractal properties (West 1990). However, one of the main drawbacks of this approach comes from the fact it is not invariant through translations, and therefore the interpretation in the case of pattern recognition applications might be more difficult. The wavelet transform is an example of coherent state decompositions used in Quantum Mechanics and renormalization group theory. The basic idea is to decompose a function into building blocks of constant shape but different size (Daubechies 1989, 1990).

Interestingly to remark a recent approach to the receptive field modeling proposed by Poggio and Girosi by using gaussian *radial basis functions* (Poggio 1989), (Girosi 1990). The radial basis function (RBF) method is well known in statistics as a possible solution to the real multivariate interpolation problem. By using a factorizable radial basis functions schema (in the case of gaussian functions), receptive fields can be readily implemented. The RBF method is closely related to pattern recognition methods as Parzen windows and potential functions (Duda 1973) and several neural network algorithms. In some sense, the use of RBF in the neural network research has come to change the classical perspective of computation performing the computations by gaussian RBF instead of threshold functions.

V. Conclusions

The Wigner distribution function (WD) is always real, encodes directly the phase information of the Fourier transformation, has a high resolution in both space and spatial frequency domains, and it is invariant within linear transformations. These are only some of the WD's characteristics that have motivated the use of this distribution in some areas of the image processing field, as in image filtering and analysis. Moreover, the WD embodies a simultaneous space-spatial frequency representation very suitable for encoding the main low-level image characteristics, including the spectral local variation. The application of the WD in several image processing tasks has been considered, specifically for filtering and analysis purposes. The previous step to obtain different results in these areas is the generation of the distribution. In this work, we have tried to present an extended vision of the different strategies of generating the WD, depending of the requirements of a particular problem. Thus, the optical Wigner processors yield an useful tool of processing where the decrease of the computer time is the more important aspect. In other cases, it may be more interesting to work without spurious noise; then digital Wigner implementations can be a good solution. In the most situations, a trade-off solution must be found between the last presented aspects, and the hybrid Wigner processor is the best solution. More recently, VLSI special purpose processors have been proposed for generating the WD and other joint representations.

Also, a discussion about the reduction of the cross-terms introduced by the bilinear nature of the definition has been considered taking account the recent results reported about this issue.

The application of the WD for texture classification and discrimination has bee considered in particular by using pairwise and multiple discriminant analysis. Several textural features have been extracted from the local spectra generated by the WD in the case of Brodatz texture. The results have been compared with the canonical Fourier spectral methods. On the other hand, the WD's texture discrimination capabilities have also been evaluated by using several pairwise texture edge detection tests.

A review about the different areas of applications of space (time)-frequency representations has been presented, emphasizing in particular the vision-oriented and detailing the specific areas in which has been considered. The importance on the use of these distributions, in the modeling of the early visual processes, has been remarked in the context of the physiological and psychophysical experiments reported in the literature.

Although there have been a lot of contributions both considering the theoretical and applicability issues, however further research is necessary to prosecute for a better knowledge about the space (time)-frequency distributions. As Cohen has recently summarized, some

problems still remain open as the consistency, i.e. to be useful in a broad range of different situations, defining of the "best" distribution and the use of non-bilinear functionals (Cohen 1989). However, the use of these distributions constitutes an excellent tool for the analysis and modeling of the neural systems, specially in the case of vision and speech application.

ACKNOWLEDGMENTS

The author is grateful to Prof. J. Feldman for providing the ICSI's facilities to support this work. I would also like to thank Prof. L. Cohen and C. Gonzalo for permitting to reproduce material related to their respective research.My gratitude to J. Bescos for his fruitful discussions and critics about the subject of this paper. I'm also grateful to A. Plaza for her general support of this work.

REFERENCES

Abeysekera, R.M.S.S. and Boashash, B. (1989), "Time-frequency domain features of ECG signals: Their application in P wave detection using the Cross Wigner-Ville Distribution", IEEE Int. Conf. on Acoust. Speech and Signal Proc., Glasgow, Scotland, 1524-1527

Adelson, E.H. and Bergen, J.R. (1985), "Spatiotemporal energy models for the perception of motion", J. Opt. Soc. Am. 2, 2, 284-299

Ashjari, B. and Pratt, W.K. (1980), "Supervised classification with singular value decomposition texture measurement", USC-IPI TR No. 860, Image Processing Institute, University of Southern California, 52-62

Asi, M.K. and Saleh B.E.A. (1990), "Time-scale modification of Speech based on the short-time Fourier transform", IEEE Trans. on Acoust., Speech and Signal Proc. (to appear)

Athale, R.A., Lee, J.N., Robinson, E.L. and Szu, H.H. (1983), "Acousto-optic processors for real-time generation of time-frequency representation", Opt. Lett. **8**, 166-168

Atlas, L. E., Loughlin, P.J., Pitton, J.W. and Fox, W.L.J. (1990), "Applications of Cone-Shaped Kernel Time-Frequency Representations to Speech and Sonar Signals", Int. Symposium on Signal Processing and its Applications, Gold Coast, Queensland, Australia (to appear)

Bajcsy, R. and Lieberman, L. (1967), "Texture gradient as a depth cue", Comput. Graphics and Image Proc. **5**, 52-67

Bamler, R. and Glünder, H. (1983a), "Coherent-optical generation of the Wigner Distribution Function of Real-Valued 2D signals", IEEE Proc. 10th. Int. Optical Computing Conf., 117-121

Bamler, R. and Glünder, H. (1983b),"The Wigner distribution function of two-dimensional signals. Coherent-optical generation and display", Optica Acta **30**, 12, 1789-1803

Bartelt, H.O., Brenner, K.H. and Lohmann, A.W. (1980), "The Wigner Distribution function and its optical production", Opt. Comm. **32**, 1, 32-38

Bastiaans, M.J. (1978), "The Wigner Distribution function applied to optical signals and systems", Opt. Comm. **25**, 26-30

Bastiaans, M.J. (1980), "Wigner Distribution function and its application to first-order optics", J. Opt. Soc. Amer. A **69**, 1710-1716

Bastiaans, M.J., (1981a), "The Wigner Distribution function of partially coherent light", Optica

Acta **28**, 1215-1224

Bastiaans, M.J. (1981b), "Signal description by means of a local frequency spectrum", Proc. SPIE **373**, "Transformations in Optical Signal Processing", 49-62

Bastiaans, M.J. (1984), "Use of the Wigner Distribution in optical problems", Proc. ECOOSA, Amsterdam, Netherlands, 251-262

Behar, J., Porat, M. and Y.Y. Zeevi (1988), "The importance of localized phase in vision and image representation", SPIE 1001, Visual Communications and Image Processing, 61-68

Berriel-Valdós, L.R., Gonzalo, C. and Bescós, J. (1988), "Computation of the Wigner Distribution Function by the Hartley Transform. Application to Image Restoration", Opt. Comm. **68**, 5, 339-344

Bescós, J. and Strand,T.C. (1978), "Optical pseudocolor encoding of spatial frequency information", Applied Optics **17**, 2524-2531.

Bescós, J., Cristóbal, G. and Santamaría, J. (1987), "Local image filtering and texture classification through the Wigner Distribution Function", Proc. Int. Commission for Optics, Quebec, 377-378

Boashash, B. (1983), "Wigner Analysis of Time-Varying Signals. An application to seismic prospecting", in Proc. Signal Proc. II: Theories and Applications, E.W. Schüssler, Elsevier Science Publishers (North Holland), Amsterdam, 703-706

Boashash, B. (1984), "High resolution signal analysis in the time-frequency domain", IEEE Int. Conf. on Computers, Systems and Signal Processing, Bangalore, India, 345-348

Boashash, B. and Escudie, B. (1985), "Wigner-Ville analysis of asymptotic signals and applications", Signal Processing **8**, 315-327.

Boashash, B. and Black, P.J. (1987), "An efficient Real-Time Implementation of the Wigner-Ville Distribution", IEEE Trans. on Acoust., Speeech and Signal Processing **35**, 11, 1611-1618

Boashash, B. and O'Shea, Peter (1988), "Application of the Wigner-Ville Distribution to the identification of machine noise", SPIE Conference, San Diego, CA, vol. 975, 209-220

Boashash, B. (ed.) (1990), "New Methods in Time-Frequency Analysis", Longman Cheshire (to appear).

Born, M. and Wolf, E. (1959), Principles of Optics, London, England, Pergamon Press.

Bovik, A.C., Clark, M. and Geisler, W.S. (1990), "Multichannel Texture Analysis using Localized

Spatial Filters", IEEE Trans. Pattern Anal. Machine Intell. **12**, 1, 55-73

Bracewell, R.N. (1983), "Discrete Hartley transform", J.Opt.Soc.Am. **73**, 1832-183

Bracewell, R.N., Bartelt, H., Lohmann, A.W. and Streibl, N. (1985), "Optical synthesis of the Hartley transform", Applied Optics **24**, 1401-1402.

Bracewell, R.N. (1986), "The Fourier transform and its applications", Mc Graw Hill, New York, 2nd. edition.

Brenner, K.H. and Lohmann, A.W. (1982), "Wigner Distribution function display of complex 1-D signals", Opt. Comm. **42**, 310-314

Brenner, K.H. (1983), "A discrete version of the Wigner Distribution function", Proc. EURASIP, Signal Processing II: Theories and Applications, 307-309

Brodatz, P. (1966), "Textures: A photographic album for artists and designers", Dover, New York

Brousil, J.K. and Smith, D.R. (1967), "A threshold logic network for shape invariance", IEEE Trans. on Ele. Computers EC-**16**, 818-828.

Buhmann, J., Lange, J. and von der Malsburg, C. (1989), "Distortion Invariant Object Recognition by Matching Hierarchically Labeled Graphs", IEEE Int. Conf. on Neural Networks, Washington D.C., 155-159

Burt, P. (1984), "The Pyramid as a Structure for Efficient Computation", in Multiresolution image processing and analysis, A. Rosenfeld (ed.), Springer, New York.

Canny, J. (1986), "A Computational Approach to Edge Detection", IEEE Trans. on Pattern Anal. Machine Intell.**8**, 6, 679-698

Carter, W.H. and Wolf, E. (1977), "Coherence and radiometry with quasihomogeneous sources", J.Opt.Soc.Am. **67**, 785-796.

Casasent, D. (1974), "A hybrid Digital/Optical Computer System", IEEE Trans. on Computers, C-**22**, 852-858.

Casasent, D. and Casasayas, F.(1975),"Optical Processing of pulsed Doppler and FM stepped radar signals", Applied Optics **14**, 1364-1372.

Casasent, D. and Psaltis, D. (1976), "Position, rotation, and scale invariant optical correlation", Applied Optics **15**, 1795-1797.

Castleman, K.R. (1979), "Digital Image Processing", Prentice Hall, Englewood Cliffs, NJ

Chan, D.S.K. (1982), "A Non-Aliased Discrete-Time Wigner Distribution for Time-Frequency

Signal Analysis", Proc. Int. Conf. Acoustics, Speech and Signal Processing, Paris, France, 1333-1336

Chester, D., Taylor, F.J. and Doyle, M. (1983), "On the Wigner Distribution", Proc. IEEE Int. Conf. on Acoust., Speech and Signal Processing, Boston, 491-494

Chester, D.B., Carney, R.R., Damerow, D.H. and Riley, C.A. (1989), "Hybrid implementation of the Wigner Distribution and other time-frequency analysis techniques", IEEE Proc. Int. Symposium on Circuits and Systems, Portland, Oregon, 1252-1255

Choi, H.I., Williams, W.J. and Zaveri, H. (1987), "Analysis of event related potentials: time frequency energy distribution", in Proc. Rocky Mountain Bioengineering Symp., 251-258

Choi, H. and Williams, W.J. (1989), "Improved time-frequency representation of multicomponent signals using exponential kernels", IEEE Trans. on Acous. Speech, Signal Processing **47**, 6, 862-871

Claasen, T.A.C.M. and Mecklenbräuker, W.F.G. (1980), "The Wigner Distribution: A tool for time-frequency signal analysis; part I: continuous-time signals", Philips J. Res. **35**, 217-250

Claasen, T.A.C.M. and Mecklenbrauker, W.F.G. (1980), "The Wigner Distribution: A tool for time-frequency signal analysis; part II: discrete time signals", Philips J. Res. **35**, 276-300

Claasen, T.A.C.M. and Mecklenbrauker, W.F.G. (1980), "The Wigner Distribution: A tool for time-frequency signal analysis; part III: relations with other time-frequency signal transformations", Philips J. Res. **35**, 372-389

Claasen, T.A.C.M. and Mecklenbräuker, W.F.G.(1983), "The Aliasing Problem in Discrete-Time Wigner Distributions", IEEE Trans. on Acoust., Speech and Signal Processing **31**, 5, 1067-1072

Cohen, L. (1966), "Generalized phase-space distribution functions", J. Math. Phys. **7**, 781-786

Cohen, L. (1976), "Quantization problem and variational principle in the phase space formulation of quantum mechanics", J. Math. Phys. **17**, 1863-1866

Cohen, L. and Posch, T.E. (1985), "Positive Time-Frequency Distributions Functions", IEEE Tran. Acoustics, Speech and Signal Processing **33**, 1, 31-37

Cohen, L. (1989), "Time-Frequency Distributions-A Review", Proc. IEEE **77**, 941-981

Combes, A., Grossman, P.H. and Tchamitchian (eds.), "Wavelets: time-frequency methods and phase space", Springer, Berlin

Conner, M. and Li, Y. (1985), "Optical generation of the Wigner distribution of signals", Applied

Optics **24**, 3825-3829.

Conners, R.W. and Harlow, C.A. (1980), "A theoretical comparison of texture algorithms", IEEE Trans. Pattern Anal. Machine Intell. **2**, 204

Cristóbal, G., Bescós, J. and Santamaría, J. (1986), "Application of the Wigner Distribution for image representation and analysis", IEEE Int. Conf. Pattern Recognition, Paris, 998-1000

Cristóbal, G., Bescós, J., Santamaría, J. and Montes, J. (1987), "Wigner distribution representation of digital images", Patt. Rec. Lett. **5**, 215-221,

Cristóbal, G., Bescós, J. and Santamaría (1989), "Image Analysis through the Wigner Distribution Function", Appl. Opt. **24**, 262-271

Cristóbal, G. (1990), "Receptive field image modeling through cellular neural networks", Summer Workshop on Analysis and Modeling of Neural Systems, Clark Kerr Campus, Berkeley, CA.

Culhane, A.D., Peckerar, M.C. and Marrian, C.R.K. (1989), "A Neural Net Approach to Discrete Hartley and Fourier Transforms", IEEE Trans. on Circuits and Systems **36**, 5, 695-703

Cutrona, L.J., Leith, E.N., Palermo, C.J. and Parcello, L.J. (1960), "Optical data processing and filtering systems", IRE Trans.Inf.Theory IT-**6**, 386-400.

Cutrona, L.J. (1965), "Recent Developments in Coherent Optical Technology", in Optical and Electro-Optical Information Processing, J.T.Tippett et al. Eds., MIT Press, Cambridge, Cap.6.

De Bruijn, N.G. (1973), "A Theory of Generalized Functions, with applications to Wigner Distribution and Weyl Correspondence", Nieuw Archief voor Wiskunde **3**, Vol. XXI, 205-280

De Valois, R. L. and De Valois K.K. (1988), "Spatial Vision", Oxford University Press, New York

Daubechies, I. (1989), "Orthonormal Bases of Wavelets with Finite Support-Connection with Discrete Filters", in Wavelets: time-frequency methods and phase space, Combes, J.M., Grossmann, A. and Tchamitchian, Ph. (eds.), Springer Verlag, New York.

Daubechies, I. (1990), "The Wavelet Transform, Time-Frequency Localization and Signal Analysis", IEEE Trans. Inform. Theory **36**, 5, 961-1005

Daugman, J.G. (1980), "Two-dimensional spectral analysis of cortical receptive fields profiles", Vision Research **20**, 847-856

Daugman, J.G. (1988), "Complete Discrete 2-D Gabor Transforms by Neural Networks for Image Analysis and Compression", IEEE Trans. on Acoust., Speech and Signal Processing **36**, 1169-

1179

Davis, L.S. and Mitchie, A. (1981), "Edge detection in textures", in Image Modeling, A. Rosenfeld (ed.), Academic Press, New York

Day, D.D. and Yarlagadda, R., "The Modified Discrete Wigner Distribution and its Application to Acoustic Well Logging", Proc. Int. Conf. on Acoustics, Speech and Signal Processing, 2713-2716

Easton, R.L., Ticknor, A.J. and Barret, H.H. (1984), "Application of the Radon transform to optical production of the Wigner distribution function", Optical Eng. **23**, 6, 738-744

Duda, R.O. and Hart, P.E. (1973), "Pattern Classification and Scene Analysis", Wiley, New York

Eichman, G. and Dong, B.Z. (1982), "Two-dimensional optical filtering of 1-D signals", Applied Optics **21**, 3152-3156.

Emerson, R.C., Citron, M.C., Vaughn, W.J. and Klein, S. A. (1987), "Nonlinear Directionality Selective Subunits in Complex Cells of Cat Striate Cortex", J. Neurophysiol. **58**, 1, 33-65

Escudie, B. (1979), "Représentation en temps et fréquence des signals d'énergie finie: analyse et observation des signaux", Ann. Télécommunic. **34**, 3-4, 101-111

Fargetton, H., Glandeaud, F. and Jourdain, G. (1979), "Filtrage dans le plan temps-frequence. Caracterisation de signaux UBF et du milieu magnetospherique", Ann.Telecommunic 34, 1/10-10/10.

Faugeras, O. and Pratt, W.K. (1980), "Decorrelation methods of texture feature extraction", IEEE Trans. Pattern Anal. Machine Intelligence **2**, 323

Field, D.J. (1986), "The structure and symmetry of simple-cell receptive-field profiles in the cat's visual cortex", Proc. R. Soc. Lond. B **228**, 379-400

Field, D.J. (1987), "Relation between the statistics of natural images and the response properties of cortical cells", J. Opt. Soc. Am. A. **4**, 12, 2379-2394

Fleet, D.J. and Jepson, A.D. (1989), "Computation of normal velocity from local phase information", IEEE Int. Conf. on Computer Vision and Pattern Recognition, San Diego, CA

Fukunaga, K. (1972), "Introduction to statistical pattern recognition", Academic Press, New York

Gabor, D. (1946), "Theory of communication", J. IEE (London) **93** (III), 429-457

Gagalowitz, A. (1981), "A new method for texture field synthesis: some applications to study of human vision", IEEE Trans. Pattern Anal. Machine Intell. **3**, 5, 520-533

Geisler, W.S. and Hamilton, D.B. (1986), "Sampling-theory analysis of spatial vision", J. Opt.

Soc. Am. A **3**, 1, 62-70

Girosi, F. and Poggio, T. (1990), "Networks and the best approximation theory", Biol. Cybern. 63, 169-176

Glünder, H.G. and Bamler, R., "Coherent optically performed operations in a 4D compound space-spatial frequency domain with applications in image analysis and quality control", Proc. SPIE **397**, "Applications of Digital Image Processing", 207-215

Gonzalez, R.C. and Wintz, P. (1987), "Digital image processing", Addison Wesley, Reading, Mass.

Gonzalo, C., Bescós, J., Berriel-Valdós, L.R. and Santamaría, J. (1989), "Space-variant filtering through the Wigner Distribution Function", Appl. Opt. **28**, 4, 730-736

Gonzalo, C., Bescós, J., Berriel-Valdós, L.R. and Artal, P. (1990), "Optical-digital implementation of the Wigner distribution function: Use in space variant filtering of real images", Appl. Opt. **29**, 17, 2569-2575

Gonzalo, C. (1990), "Use of the 4-D Discrete Wigner Distribution Function in simulation and restoration of space variant degraded images", Appl. Opt., (submitted).

Goodman, J.W. (1968), "Introduction to Fourier Optics", McGraw-Hill, New York.

Grossmann, A. and Morlet, J. (1984), "Decomposition of Hardy functions into square integrable wavelets of constant shape", SIAM J. Math. **15**, 723-736

Gupta, A.K. and Asakura, T. (1986), "New optical system for the efficient display of Wigner distribution function using a single object transparency", Optics Communications **60**, 265-268.

Haralick, R.M. (1979), "Statistical and structural approaches to texture", Proc. IEEE **67**, 5, 786-804

Hartley, R.V.L. (1042), "A more symmetrical Fourier analysis applied to transmission problems", Proc. IRE **30**, 144-150.

Hawken, M.J. and Parker, A.J. (1987), "Spatial properties of neurons in the monkey striate cortex", Proc. R. Soc. Lond. B **231**, 251-288

Heeger, D. (1987), "Model for the extraction of image flow", J. Opt. Soc. Am. A **4**, 8, 1455-1471

IMSL (1982), International Mathematical and Statistical Libraries, IMSL Inc., Houston, TX

Hopkins, H.H. (1955), "The frequency response of a defocused optical system", Proc. R.Soc.London Ser.A **231**, 91-103.

Huang, T.S. and Kasnitz, H.L. (1967), Proc. Soc. Photo and Instru. Engrs., Seminar Computerized Imaging Techniques.

Hubel, D. and Wiesel, T. (1962), "Receptive field, binocular interaction, and functional architecture in the cat's visual cortex", J. Physiol. (London) **160**, 106-154

Imberger, J. and Boashash, B. (1986), "Application of the Wigner-Ville Distribution to Temperature Gradient Microstructure: A new technique to study small-scale variations", J. Phys. Oceanogr. **16**, 12, 1997-2012

Jacobson, L. and Wechsler, H. (1982a), "The Wigner Distribution as a tool for deriving an invariant representation of 2-D images", Proc. Int. Conf. on Pattern Recognition and Image Processing, Las Vegas, 218-220

Jacobson, L and Wechsler, H. (1982b), "The Wigner Distribution and its usefulness for 2-D image processing", Proc. Int. Conf. on Pattern Recognition, Munich, Germany, 538-541

Jacobson, L. and Wechsler, H. (1983), "The composite Pseudo Wigner Distribution (CPWD): a computable and versatile approximation to the Wigner Distribution (WD), Proc. Int. Conf. on Acoustics, Speech and Signal Proc., Boston, 254-256

Jacobson, L. and Wechsler, H. (1984), "A theory for invariant object recognition in the frontoparallel plane", IEEE Trans. Pattern Anal. Machine Intell., **6**, 325-331

Jacobson, L. and Wechsler, H. (1987), "Derivation of Optical Flow using a Spatiotemporal-Frequency approach", Comp. Vision, Graphics and Image Proc. **38**, 29-65

Jacobson, L. and Wechsler, H. (1988), "Joint spatial/spatial-frequency representations", Signal Proc. **14**, 1, 37-68

Jain, A.K. (1989), "Fundamentals of Digital Image Processing", Prentice Hall, Englewood Cliffs, N.J.

Janse, C.P. and Kaizer, A.J.M. (1983), "Time-Frequency Distributions of Loudspeakers: The Application of the Wigner Distribution", J. Audio Eng. Soc. **31**, 4, 198-223

Janssen, A.J.E.M. and Claasen, T.A.C.M. (1985), "On positivity of Time-Frequency Distributions", IEEE Trans. on Acoust., Speech and Signal Processing **33**, 4, 1029-1032

Jau, Y.C. and Chin, R.T. (1988), "Shape from texture using the Wigner Distribution", Proc. IEEE Int. Conf. on Computer Vision and Pattern Recognition, Ann Arbor, Michigan, 515-523

Jenkin, M.R.M. (1988), "Visual stereoscopic computation", Ph.D. Thesis, Dept. of Computer Science. University of Toronto, Toronto, Ontario, Canada

Jernigan, M.E. and D'Astous, F. (1984), "Entropy-Based Texture Analysis in the Spatial Frequency Domain", IEEE Trans. on Pattern Anal. Machine Intell. **6**, 2, 237-243

Jones, J. and Palmer L. (1987), "An evaluation of the two-dimensional Gabor filter model of simple receptive fields in cat striate cortex", J. Neurophys. **58**, 1233-1258

Julesz, B. and Bergen, J.R. (1983), "Textons, the fundamental elements in preattentive vision and perception of textures", Bell Syst. Tech. J. **62**, 2, 1619-1645

Kay, R. and Matthews, D. (1972), "On the existence in human auditory pathways of channels selectively tuned to the modulation present in frequency-modulated tones", J. Physiol. **225**, 657-677

Kay, S. and Boudreaux-Bartels, G.F. (1985), "On the optimality of Wigner distribution for detection", IEEE Int. Conf. on Acoustics, Speech, and Signal Processing, 1017-1020.

Kirkwood, J.G. (1933), "Quantum statistics of almost classical ensembles", Phys. Rev. **44**, 31-37

Koenderink, J.J. and van Doorn, A.J. (1990), "Receptive field families", Biol. Cybern. 63, 291-297

Kovasznay, L.S.G. and Joseph, H.M. (1953), "Processing of two-dimensional patterns by scanning techniques", Science **118**, 475-477

Kronland-Martinet, R., Morlet, J. and Grossmann, A. (1987), "Analysis of sounds patterns through wavelet transforms", Int. J. of Pattern Recognition and Artificial Intelligence **1**,2 , 273-302

Kruger, R.P., Thompson, W.B. and Turner, A.F. (1974), "Computer Diagnosis of Pneumoconiosis", IEEE Trans. Sys. Man Cyber. SMC-**4**, 40-49

Kumar, B.V.K.V. and Carroll (1983), "Pattern recognition using Wigner Distribution Function", in IEEE Proc. 10th Int. Optical Computing Conf., 130-135

Kumar, B.V.K.V. and Carrol, C.W. (1984), "Effects of sampling on signal detection using the Cross-Wigner distribution function", Applied Optics, 23, 4090-4094.

Lendaris, G.G. and Stanley, G.L. (1977), "Diffraction Pattern Sampling for Automatic Pattern Recognition", in Computer Methods in Image Analysis, Aggarwal, J.K., Duda, R.O. and Rosenfeld, A. (eds.), Los Angeles, IEEE Computer Society

Li, Y., Eichmann, G. and Conner, M. (1988), "Optical Wigner distribution and Ambiguity function for complex signals and images", Optics Communications 67, 177-179.

Lizuka, K. (1983), "Engineering Optics", Optical Sciences Series, Springer Verlag, Berlin, Heidelberg, New York, Tokyo, Cap.11.

Malik, J. and Perona, P. (1989), "A computational model of texture segmentation", IEEE Int. Conf. on Computer Vision and Pattern Recognition, San Diego, CA, 326-332

Mallat, S.G. (1989a), "A theory for multiresolution signal decomposition: the wavelet representation", IEEE Trans. Pattern Anal. Machine Intell. **11**, 7, 674-693

Mallat, S.G. (1989b), "Multifrequency channel decompositions of images and wavelet models", IEEE Trans. Acous. Speech, Signal Processing **37**, 12, 2091-2110

Marcelja, S. (1980), "Mathematical description of the responses of simple cortical cells", J. Opt. Soc. Am.A **70**, 11, 1297-1300

Mark, W.D. (1970), "Spectral analysis of the convolution and filtering of non-stationary stochastic processes", J. Sound Vib. **11**, 19-63

Marks II, R.J., Walkup, J.F. and Krile, T.F. (1977), "Ambiguity function display: an improved coherent processor", Applied Optics **16**, 746-750.

Marks II, R.J. and Hall, M.W. (1979), "Ambiguity function display using a single input.", Applied Optics **18**, 2539-2540.

Marr, D. and Hildred, E. (1980), "Theory of edge detection", Proc. Royal Soc. of London B **207**, 187-217

Martens, J.B. (1990a), "The Hermite Transform-Theory", IEEE Trans. on Acoustics, Speech and Signal Processing 38, 9, 1595-1606

Martens, J.B. (1990b), "The Hermite Transform-Applications", IEEE Trans. on Acoustics, Speech and Signal Processing 38, 9, 1607-1618

Mateeva, T. and Sharlandjiev, P. (1986), "The generation of a Wigner Distribution Function of Complex Signals by Spatial filtering", Opt. Comm. **57**, 153-155

Martin, W. and Flandrin, P. (1985a), "Detection of changes of signal structure using the Wigner-Ville Spectrum", Signal Proc. **8**, 215-233

Martin, W. and Flandrin, P. (1985), "Wigner-Ville Spectral Analysis of Nonstationary Processes", IEEE Trans. on Acoust., Speech and Signal processing **33**, 6, 1461-1469

Møller, A. (1978), "Coding of time-varying sounds in the cochlear nucleus", Audiology **17**, 446-468

Morrone, M.C. and Burr, D.C. (1988), "Feature Detection in human vision: a phase-dependent energy model", Proc. R. Soc. Lond. B **235**, 221-245

Movshon, J. A., Thompson, I.D. and Tolhurst, D.J. (1978), "Spatial summation in the receptive fields of simple cells in the cat's striate cortex", J. Physiol. London **283**, 53-77

Oppenheim, A. V. and Lim, J.S. (1981), "The importance of phase in signals", Proc. IEEE **69**, 5, 529-541

Pacut, A., Kolodziej, W.J. and Said, A., "Discrete Domain Wigner Distributions- A Comparison and an Implementation", Proc. IEEE Int. Symposium on Circuits and Systems, Portland, Oregon, 1264-1267

Page, C.H. (1952), "Instantaneous Power Spectra", J. Appl. Phys. **23**, 103-106

Paler, K. and Bowler I.W. (1986), "Gabor Filters applied to Electronic Speckle Pattern Interferometer Images", IEE Int. Conf. on Image Processing and its applications. Imperial College, U.K., 258-262

Perry, A. and Lowe, D.G. (1989), "Segmentation of textured images", IEEE Int. Conf. on Computer Vision and Patt. Recogn., San Diego, CA, 319-325

Peyrin, F. and Prost, R. (1986), "A Unified Definition for the Discrete-Time, Discrete-Frequency, and Discrete-Time/Frequency Wigner Distributions", IEEE Trans. on Acoust., Speech and Signal Processing **34**, 4, 858-867

Pollen, D. and Ronner, S. (1981), "Visual Cortical Neurons as Localized Spatial Frequency Filters", IEEE Trans. on Systems, Man and Cybernetics **13**, 5, 907-916

Poggio, T. and Gorosi, F. (1989), "A theory of networks for approximation and learning", M.I.T. A.I. Memo No. 1140

Porat, M. and Zeevi, Y.Y. (1988), "The generalized scheme of image representation in biological and machine vision", IEEE Trans. Pattern Anal. Machine Intell. **10**, 4, 452-467

Porat, M. and Zeevi, Y.Y. (1989), "Localized Texture Processing in Vision: Analysis and Synthesis in the Gaborian Space", IEEE Trans. on Biomedical Eng. **36**, 1, 115-129

Ratliff, F. (1965), "Mach Bands: Quantitative studies on Neural Networks in the Retina", Holden Day, San Francisco.

Read, P.R. and Treitel, S. (1973), "The stabilization of two-dimensional recursive filters via the discrete Hilbert transform", IEEE Trans. Geosci. Electron. **GE-11**, 153-207

Reed, T. and Wechsler, H. (1988), "Texture analysis and clustering using the Wigner Distribution", Proc, 9th. Int. Conf. on Pattern Recognition, Rome, Italy, 770-772

Reed, T.R. and Wechsler, H. (1990), "Segmentation of Textured Images and Gestalt Organization using spatial/spatial-frequency representations", IEEE Trans. Pattern Anal. Machine Intell. **12**, 1, 1-12

Rihaczek, A.W. (1968), "Signal Energy Distributions in Time and Frequency", IEEE Trans. Inform. Theory **14**, 369-374

Riley, M.D.(1989), "Speech time-frequency representations", Kluwer Academic Publishers, Boston, Mass.

Saleh, B.E.A. and Subotic, N.S. (1985), "Time-variant filtering of signals in the mixed time-frequency domain", IEEE Tran. ASSP **33**, 6, 1479-1485

Sanger, T.D. (1988), "Stereo disparity computation using Gabor filters", Biol. Cybern. **59**, 405-418

Stark, H. (1982), "Applications of optical Fourier transforms", Academic Press, New York

Subotic, N.S. and Saleh, B.E.A. (1984a), "Optical time-variant processing of signals in the mixed time-frequency domain", Opt. Comm. **52**, 4, 259-264

Subotic, N.S. and Saleh, E.A. (1984b), "Generation of the Wigner distribution function of two-dimensional signals by a parallel optical processor", Optics Letters **9**, 471-473.

Sun, M., Li, C.C., Sekhar, L.N. and Sclabassi, R.J. (1989a), "Efficient Computation of the Discrete Pseudo-Wigner Distribution", IEEE Trans. on Acoustics, Speech and Signal Processing **37**, 11, 1735-1742

Sun, M., Li, C.C., Sekhar, L.N. and Sclabassi, R.J. (1989b), "Elimination of cross-components os the discrete Pseudo Wigner Distribution via image processing", IEEE Int. Conf. on Acoust., Speech and Signal Processing, Glasgow, Scotland, 2230-2233

Sutton, R.N. and Hall, E.L. (1972), "Texture Measures for Automatic Classification of Pulmonary Disease", IEEE Trans. Computers **21**, 667-676

Szu, H.H (1982), "Two-dimensional optical processing of one-dimensional acoustic data", Optical Engineering **21**, 804-813.

Tabernero, A. and Navarro, R. (1990), "Performance of Gabor functions for Texture Analysis", submitted to IEEE Trans. Pattern Anal. Machine Intell.

Tan, T.N. and Constantinides, A.G. (1990), "Texture Analysis Based on A Human Visual Model", IEEE Int. Conf. on Acoustics, Speech and Signal Processing, Albuquerque, NM, 2137-2140

Tanimoto, S.L., Ligocki, T.L and Ling R. (1987), "A Prototype Pyramid Machine for Hierarchical Cellular Logic", in Parallel Computer Vision, L. Uhr (ed.), Academic Press, Orlando, Fa

Usui, S. and Araki, H. (1990), "Wigner Distribution Analysis of BSPM for optimal sampling", IEEE Engin. in Medicine and Biology **9**, 1, 29-32

Van Essen, D.C. and C. Anderson (1990), "Information processing strategies and pathways in the primate retina and visual cortex", in Introduction to Neural and Electronic Networks, Zornetzer, S.F., Davis J.L. and Lau, C. (eds.), Academic Press, Orlando, Florida

Van Gool, L. Dewaele, P. and Oosterlink, A. (1985), "Texture Analysis Anno 1983", Computer Vision, Graphics and Image Processing **29**, 336-357

Ville, J. (1948), "Théorie et applications de la notion de signal analitique", Cables et Transmission **2A**, 61-74

Waibel, A. (1989), "Modular Construction of Time-Delay Neural Networks for Speech Recognition", Neural Computation **1**, 39-46

Walther, A. (1968), "Radiometry and Coherence", J.Opt.Soc.Am. **58**, 1256-1259.

Walther, A. (1973), "Radiometry and Coherence", J.Opt.Soc.Am. **63**, 1622-1623.

Weber, A.G. (1989), "Image Data Base", Signal and Image Processing Institute, University of Southern California, Los Angeles, CA

Webster, M.A. and de Valois, R.L. (1985), "Relationship between spatial-frequency and orientation tuning of striate-cortex cells", J. Opt. Soc. Am. A **2**, 1124-1132

West, B.J. (1990), "Sensing scaled scintillations", Special issue on Fractals in the Imaging Sciences, J. Opt. Soc. Am. A 7, 6, 1074-1100

Weszka, J.S., Dyer C.R. and Rosenfeld, A. (1976), "A comparative study of texture measures for terrain classification", IEEE Trans. Syst. Man Cybern. **6**, 269-285

Wigner, E. (1932), "On the Quantum Correction for Thermodynamic Equilibrium", Phys. Rev. **40**, 749-759

Williams, W.J. and Jeong, J. (1989), "New time-frequency distributions: theory and applications", Proc. Int. Symp. on Circuits and Systems, Portland, Oregon, 1243-1247

Woodward, P.M. (1953), "Probability and Information Theory with Application to Radar".

London, England: Pergamon

Young, R.A. (1985), "The gaussian derivative theory of spatial vision: analysis of cortical cell receptive field line-weighting profiles", General Motors Rep. No. GMR-4920, Warren, Michigan

Young, R.A. (1987), "The gaussian derivative model for spatial vision: I. Retinal mechanisms", Spatial Vision **2**, 4, 273-293

Zeevi, Y.Y. and Porat, M. (1988), "Computer image generation using elementary functions matched to human vision", in Theoretical foundations of Computer Graphics, R.E. Earnshaw, Ed., NATO ASI Series **40**, Springer, Berlin, 1197-1241

Zhao, Y., Atlas, L. and Marks II, R. (1990), "The use of Cone-Shaped Kernels for Generalized Time-Frequency Representations of Nonstationary Signals", IEEE Trans. on Acoustics, Speech and Signal Processing **38**, 7, 1084-1091.

Zheng, C., Wildmalm, S.E. and Williams, W.J. (1989), "New time-frequency analysis of EMG and TMJ sound signals", IEEE Int. Conf. on Engineering in Medicine and Biology, 741-742

Zhu, Y.M., Goutte, R. and Peyrin, F. (1990a),"On the use of 2-D analytic signals for Wigner analysis of 2-D real signals", IEEE Int. Conf. Acoust., Speech and Signal Proc., Albuquerque NM, 1989-1992

Zhu, Y.M., Peyrin, F. and Goutte, R. (1990b), "The use of a two dimensional Hilbert transform for Wigner analysis of 2-dimensional real signals", Signal Proc. **19**, 205-220

Appendix I

Captions of figures

Figure 2.1: a) Sinusoidal grating object of 64 pixels/period; b) WD of a) for the x direction and the autoconvolution profile (ω=0) with zoom x 2.

Figure 2.2: Composite rectangular grating of 32, 16 and 8 pixels/period. Reprinted by permission from (Gonzalo 1989).

Figure 2.3: Representation of the function f(n+k) f^*(n-k). The spatial variable n is represented along the horizontal axis and the k parameter along the vertical axis. Reprinted by permission from (Gonzalo 1989).

Figure 2.4: Discrete Wigner distribution function of Fig. 2.2. The spatial variable n is mapped along the horizontal axis and the frequency variable along the vertical axis. Reprinted by permission from (Gonzalo 1989).

Figure 2.5: WD for a rectangular window test in the y direction and the autoconvolution profile (ω=0) with zoom x 2.

Figure 2.6 a) Rectangular grating test; b) recovered image from the discrete DW results of local digital filtering operations: low-pass filtering (half left) an filtering (half right).

Figure 2.7: Hybrid Wigner optical digital processor used to obtain space variant filtered images. L_1 Fourier transforms the shifted image f(x+x_0/2,y+y_0/2). The mirror *M* reflected its spectrum, and L_2 yields f(x-x_0/2,y-y_0/2) performs the Fourier transform of the product function of the two images and L_3 inverses it

Figure 3.2: a) Preprocessed Brodatz textures (clockwise from top left): sand, straw, raffia and cotton canvas; b) Fourier spectra associated to each texture of Fig. 3.2a.

Figure 3.4: a) Product images corresponding to cotton canvas texture at points (128,112), (128, 114),..., (128,142) (origin at top left); b) WD associated to these points.

Figure 3.5: a) Product images corresponding to straw texture at points (128,112), (128, 114),..., (128,142) (origin at top left); b) WD associated to these points.

Figure 3.6: a) Two dimensional scatter diagram associated with the Fourier spectral energy measures; b) Id. for the co-ocurrence method and c) Id. for the WD method.

Figure 3.7: a) Cotton canvas-raffia texture Brodatz pair; b) (from left to right and top to bottom) WD associated to the points (128,112), (128, 114),..., (128,142).

Figure 3.8: Results of the edge detection mechanism by using the WD. The plots represent the edge operator versus the interpixel distance along a line perpendicular to the texture border: a) sand-straw pair; b) straw-raffia pair; c) cotton canvas-raffia pair; d) sand-cotton canvas pair. The range of e_W has been normalized.

Figure 4.1: a). 1-D even-Gabor function corresponding to the signal $f(x) = exp\,[-\pi\,((x-32)^2/144)]\cos\,[0.6666\pi\,(x-32)]$ b). 1-D odd-Gabor function corresponding to the function $f(x) = exp\,[-\pi\,((x-32)^2/144)]\sin\,[0.6666\pi\,(x-32)]$

Figure 4.2:Analytic signal associated to the Gabor functions represented in Fig.4.1a and Fig. 4.1b. This helicoidal pattern resembles the *momentum states*'s description in Quantum Mechanics, giving an harmonic description in terms of *pure tones* corresponding to different moment values that a particle might have. The projections of this helicoidal pattern onto the XY and YZ planes correspond to the even and odd Gabor functions respectively.

Figure 4.3 a). Basic wavelet function corresponding to a second derivative of a Gaussian function $f(x) = (2/(\sqrt{3}))\,\pi^{-1/4}\,(1-x^2)\,exp\,(-x^2/2)$. This transform is often called the *mexican hat* for its form.b). Example of wavelet associated to the previous function; it can be obtained by a translation of x'=3+x/4 and by a reducing scale factor of 0.5. c) Id. by a translation of x'=2x-15 and a scale factor of $\sqrt{2}$.

Cristobal Fig 2 ×20 15 Jan 80

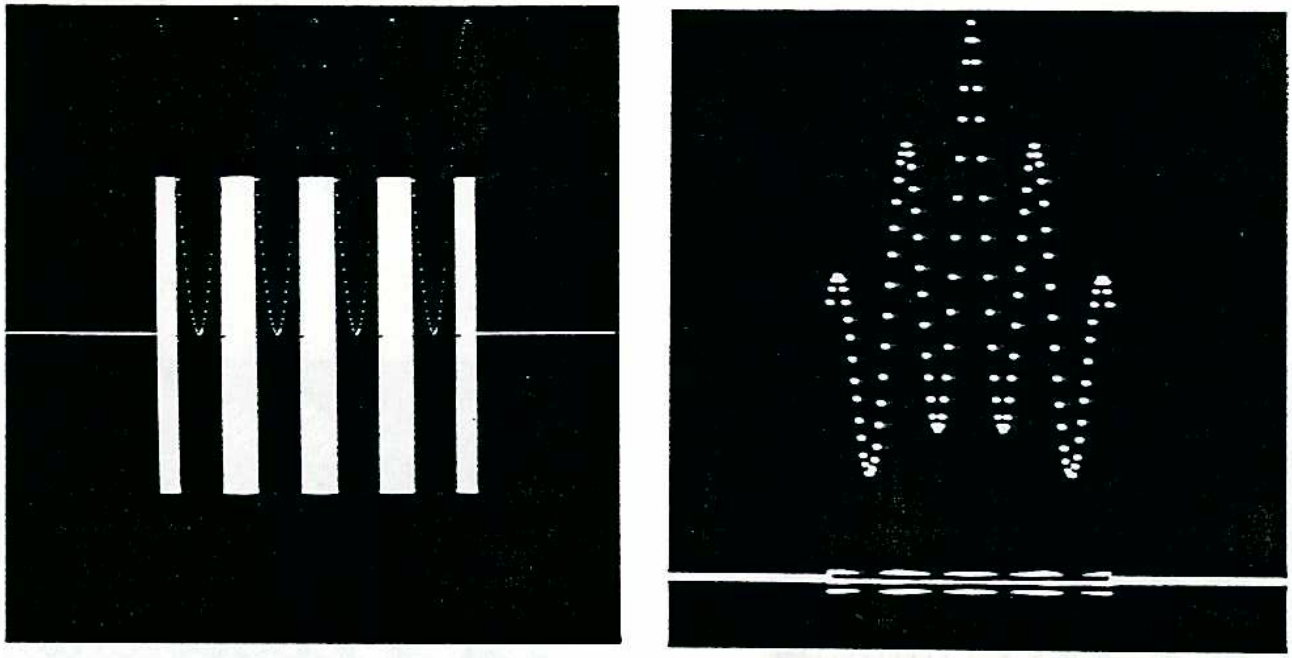

a b

Fig. 2.1

JRL Optic ISSUE Jan 15 KB 18 FIG 2

50½ % OF ORIG _____ DENSITOMETER

mw

#94551-PO-6-8/88-25M

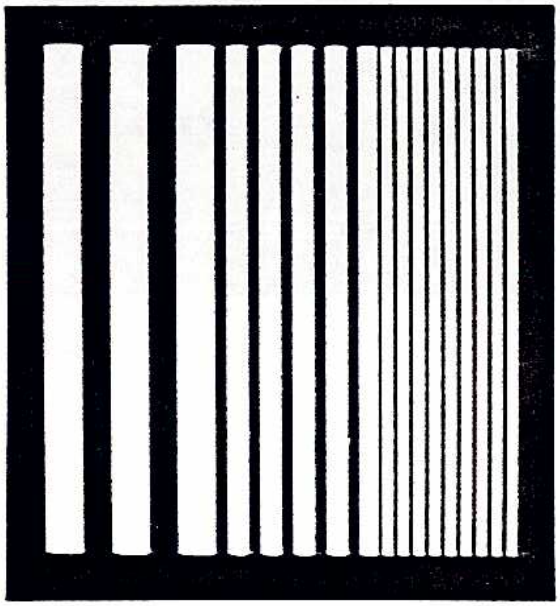

Fig. 2.2

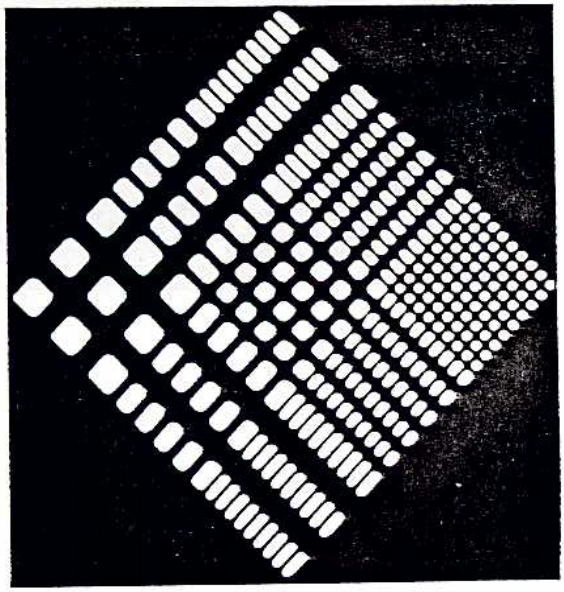

Fig. 2.3

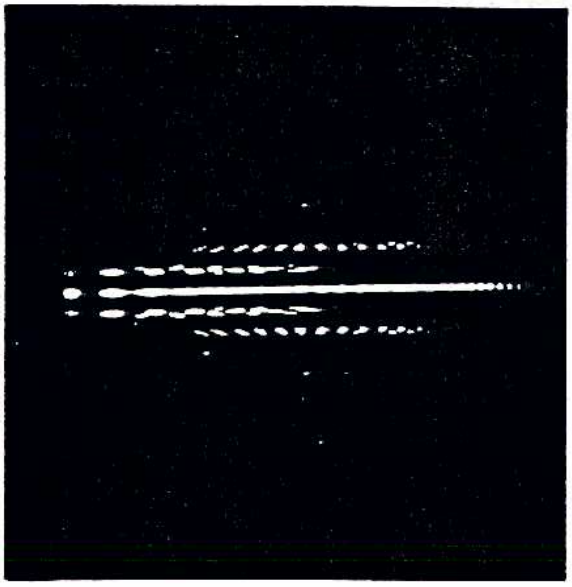

Fig. 2.4

Cristobal Fig 5 × 20 15 Jan 90

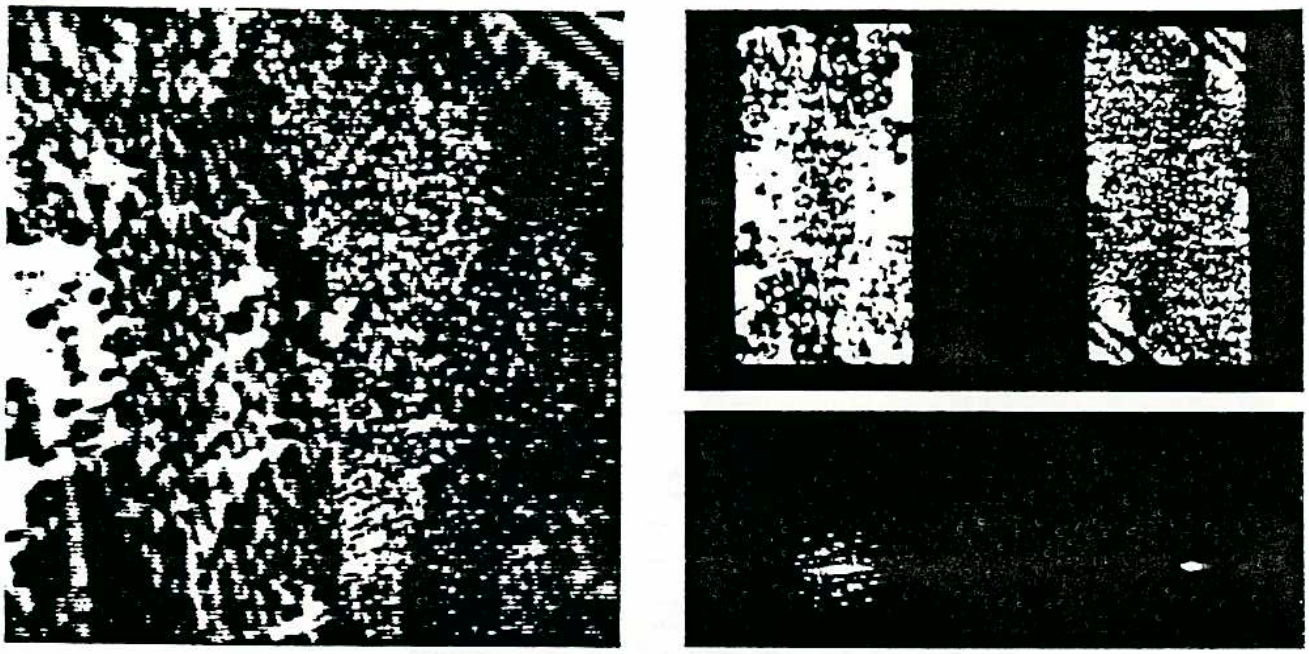

a b

Fig. 2.6

Cristobal F'd 15 Jan
1 ←—— X 13 —— A0 →1

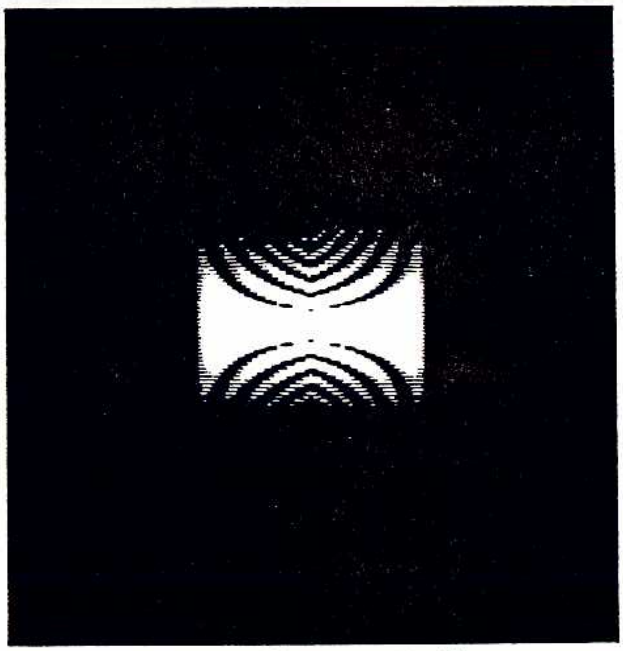

Fig. 2.5

JRL Optics ISSUE Jan 15 KB 18 FIG 4
67½ % OF ORIG _____ DENSITOMETER
mw

#94551-PO-6-8/88-25M

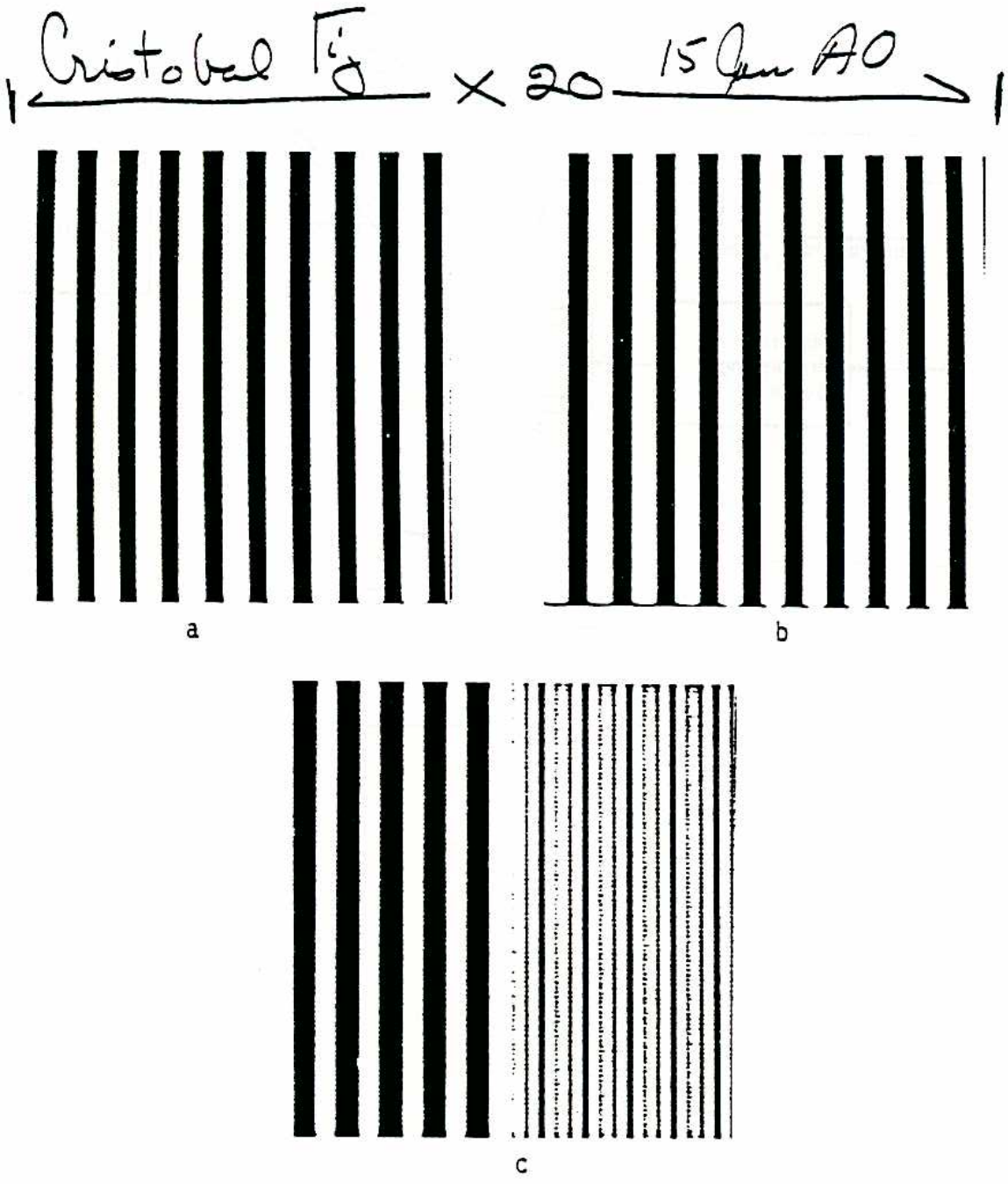

Fig. 2.7

JRL Optic ISSUE Jan 15 KB 18 FIG 7

58½ % OF ORIG _____ DENSITOMETER

MW

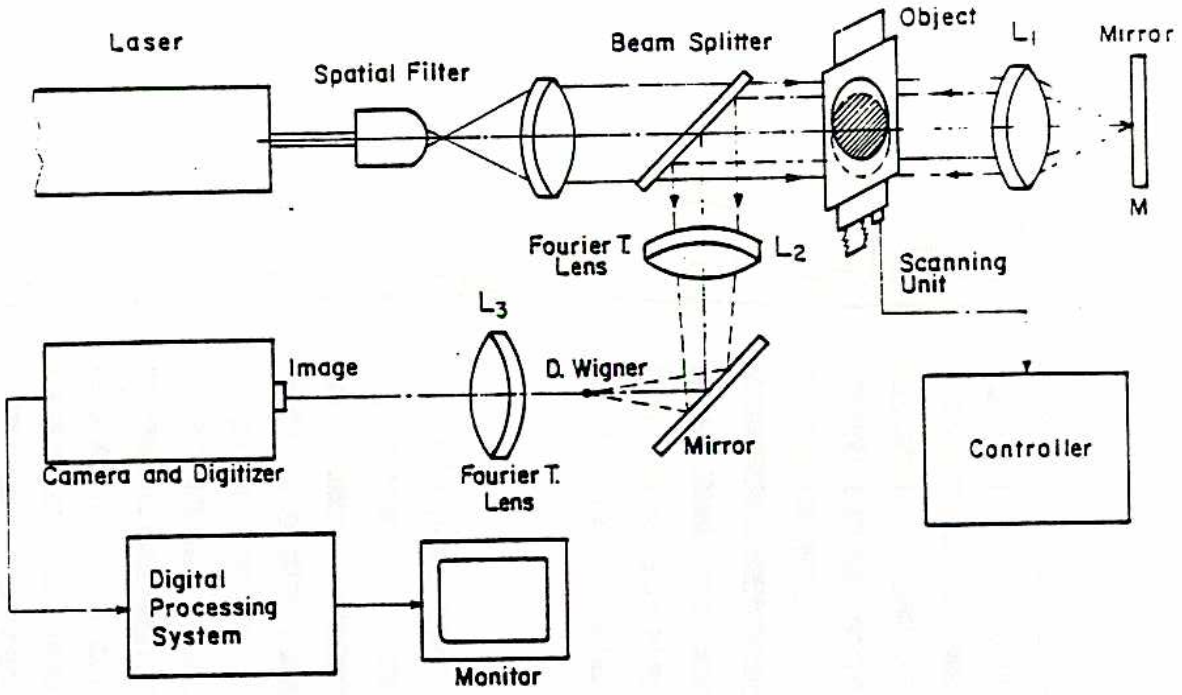
Laser
Spatial Filter
Beam Splitter
Object
L_1
Mirror
M
Fourier T. Lens
L_2
Scanning Unit
L_3
Image
D. Wigner
Mirror
Controller
Camera and Digitizer
Fourier T. Lens
Digital Processing System
Monitor

Fig. 2.8

Critobal Fig × 20 15 Jm AO

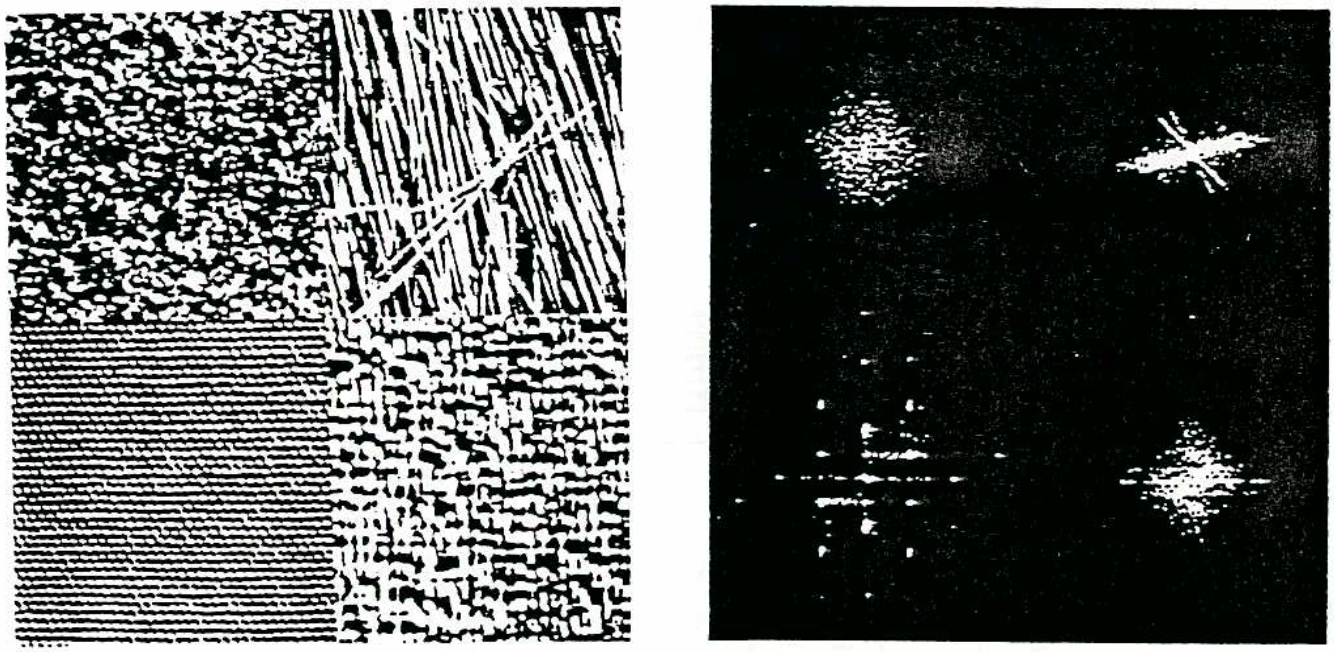

a b

Fig. 3.2

JRL Optic ISSUE Jan 15 KB 18 FIG 8

48 3/4 % OF ORIG _____ DENSITOMETER

MW

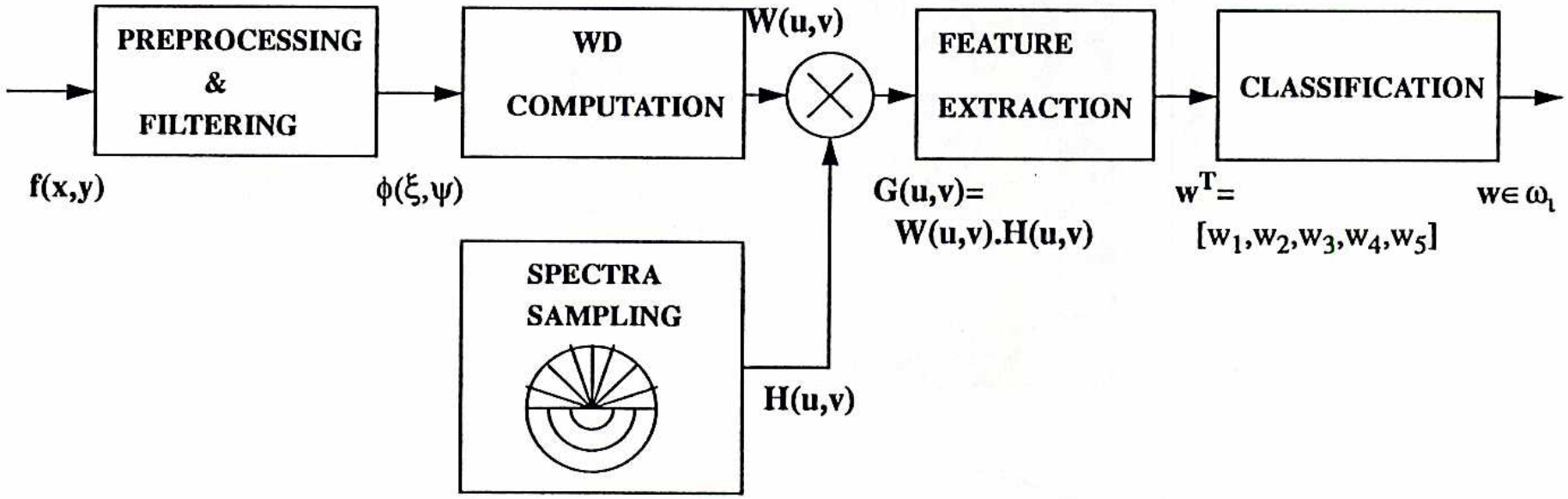

Figure 3.3. The scheme shows the different process involved in the image analysis application through the WD, from the raw data f(x,y) to the categorization process $w \in \omega_i$

Cristobal Fig ×20 15 Jan 70

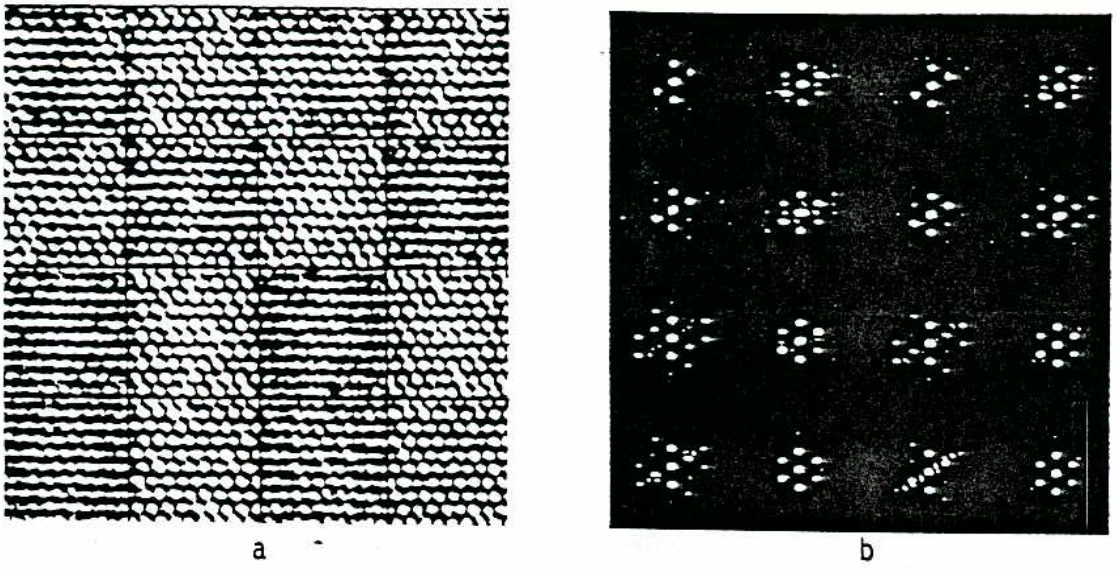

a b

Fig. 3.4

Cristobal Fig ×20 15 Jan 70

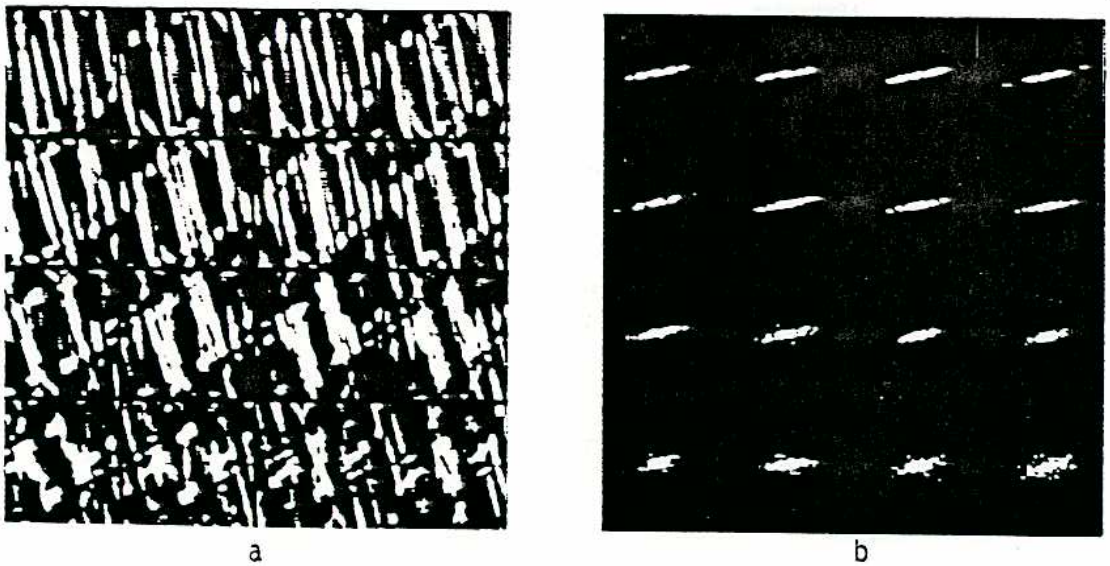

a b

Fig. 3.5

JRL Optic ISSUE Jan 15 KB 18 FIG 10

59 % OF ORIG _____ DENSITOMETER

MW

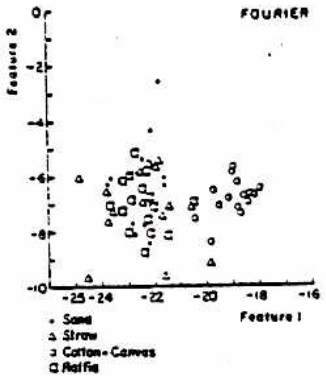

Fig. 3.6a

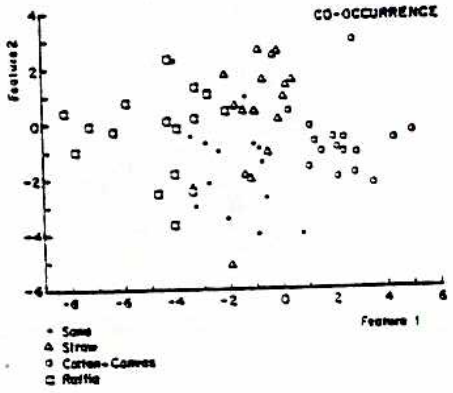

Fig. 3.6b

Cristobal Falls ×20 15 Jan AO

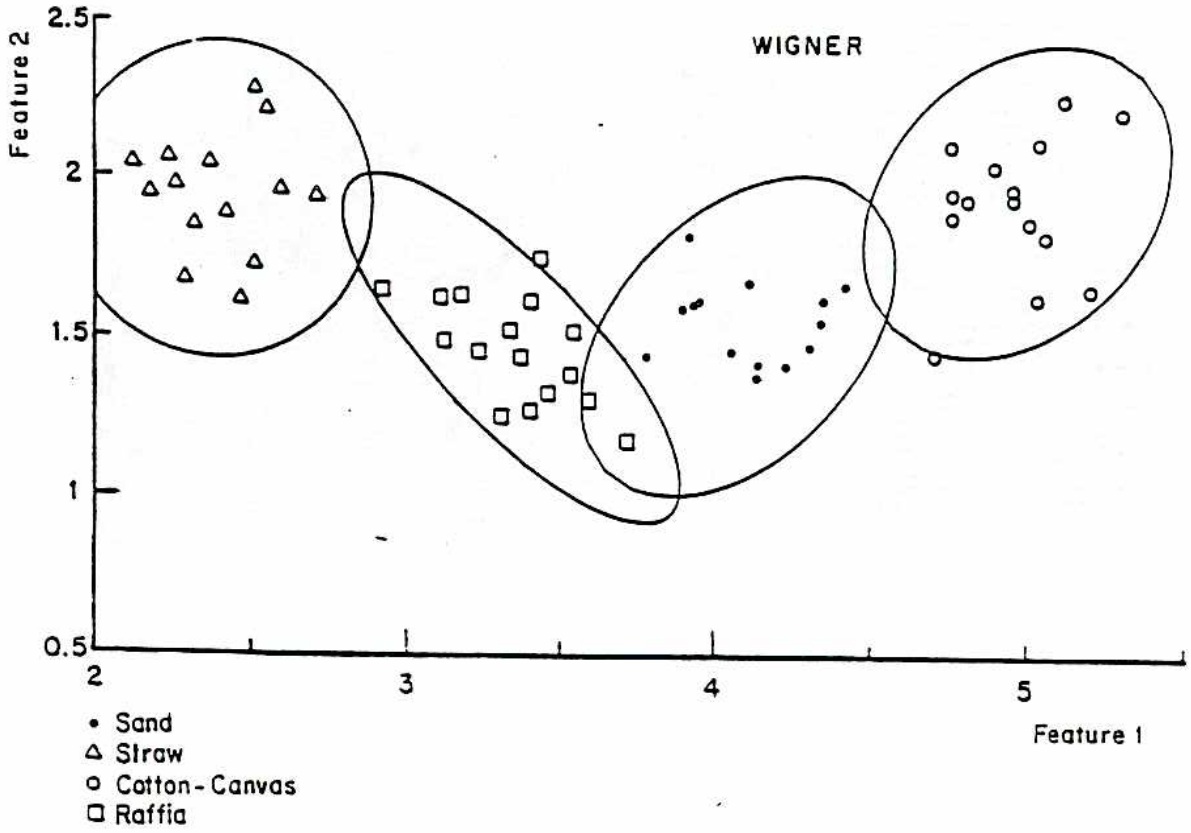

JRL Optic ISSUE Jan 15 KB 18 FIG 11C

54½ % OF ORIG _____ DENSITOMETER

mw

#94551-PO-8-8/88-25M

Fig. 3.6c

Critobal Fig × 20 15 Jan 90

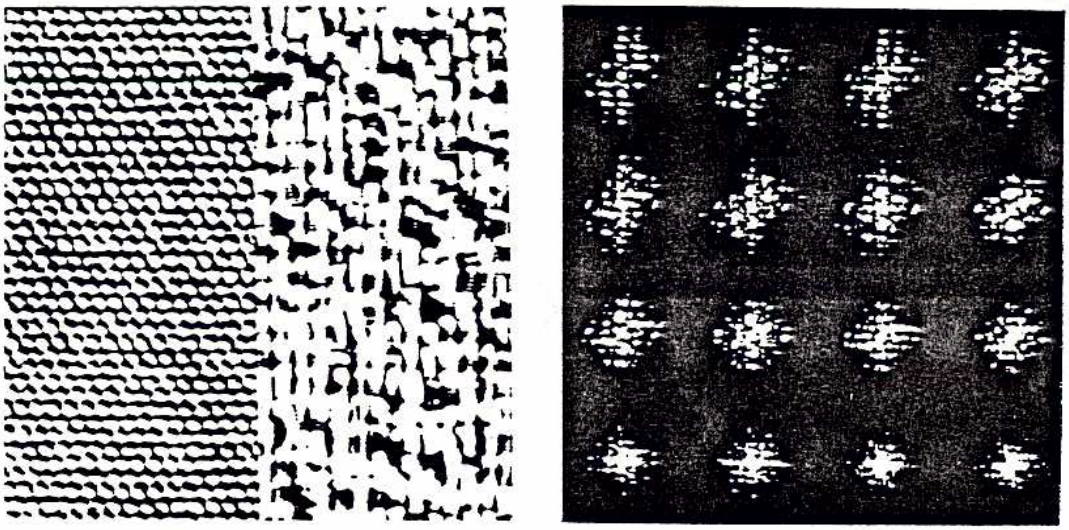

a b

JRL Optics ISSUE Jan 15 KB 18 FIG 12

61 % OF ORIG _____ DENSITOMETER

MW

#94551-PO-6-8/88-25M

Fig. 3.7

Cristobal 15 Jan 80
← X13 →

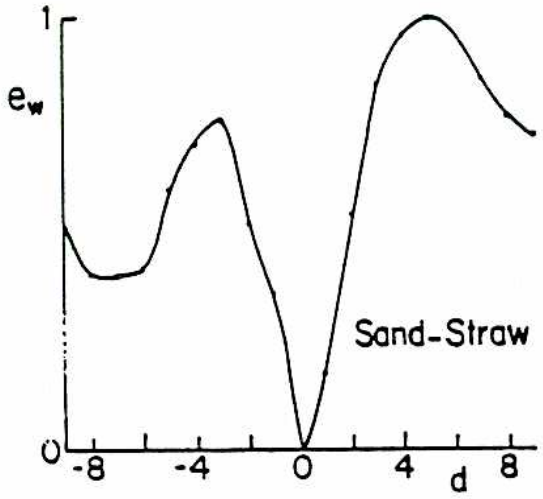

Fig. 3.8a

a

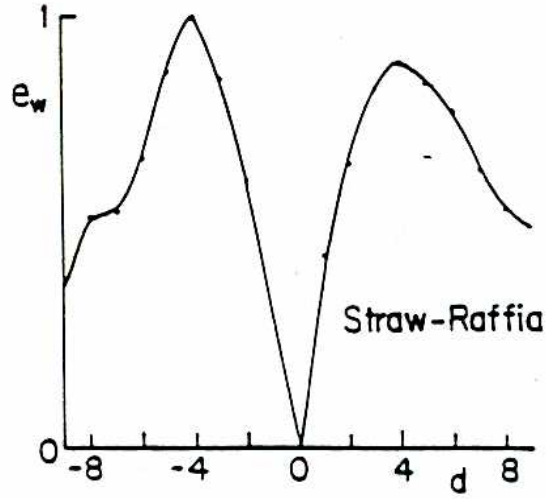

Fig. 3.8b

b

JRL Optics ISSUE Jan 15 KB 18 FIG 13a, b

Cristobel 15 Jun A0

×13

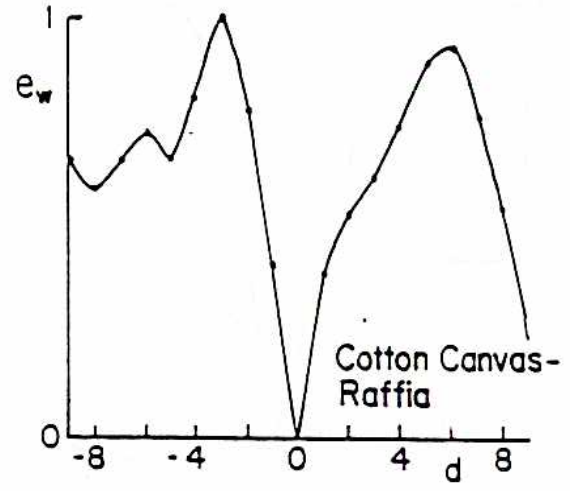

Fig. 3.8c

c

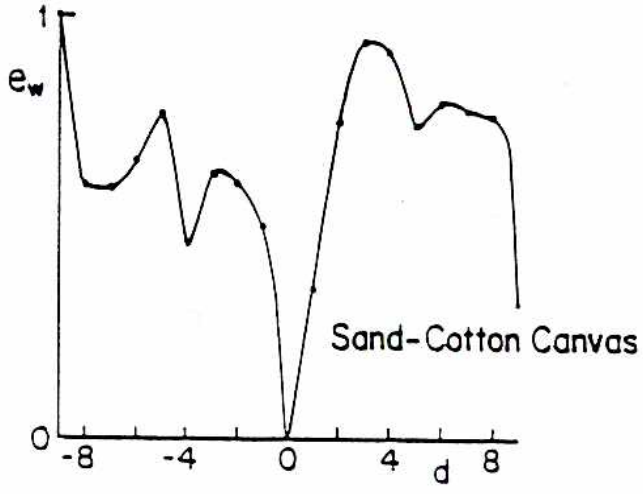

Fig. 3.8d

d

JRL Optic ISSUE Jan 15 KB 18 FIG 13C, d

62 % OF ORIG DENSITOMETER

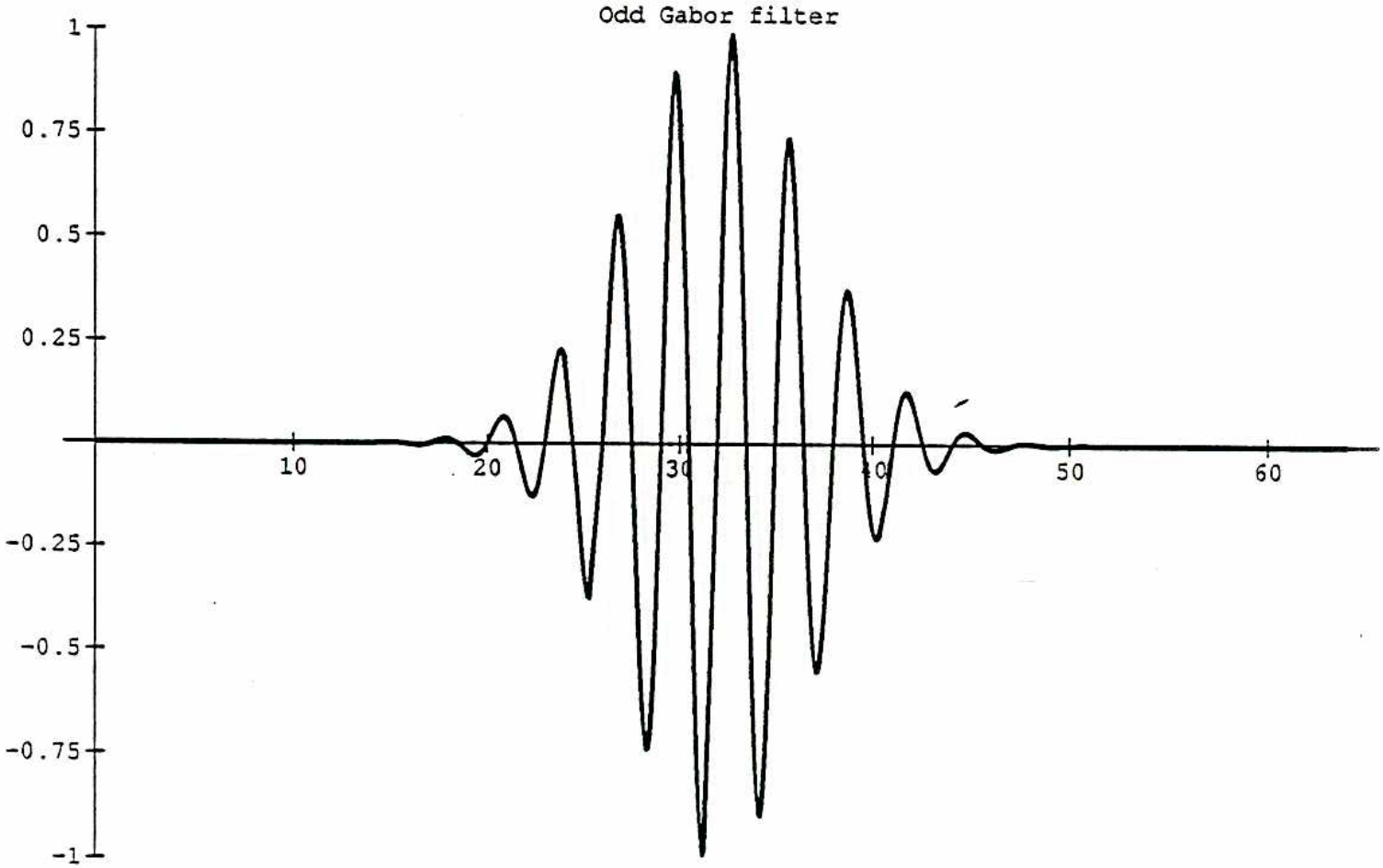

Fig. 4.1a

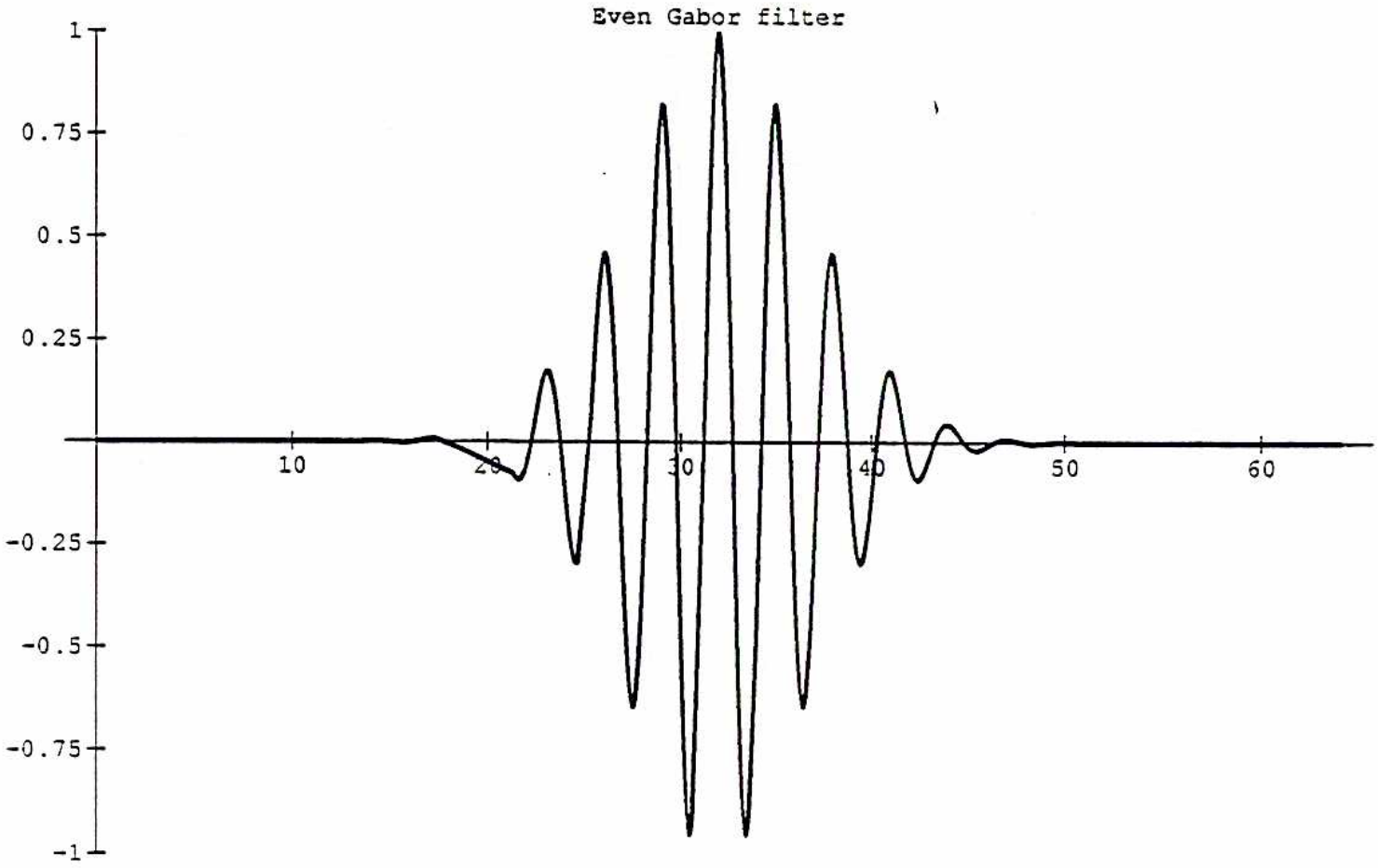

Fig. 4.1b

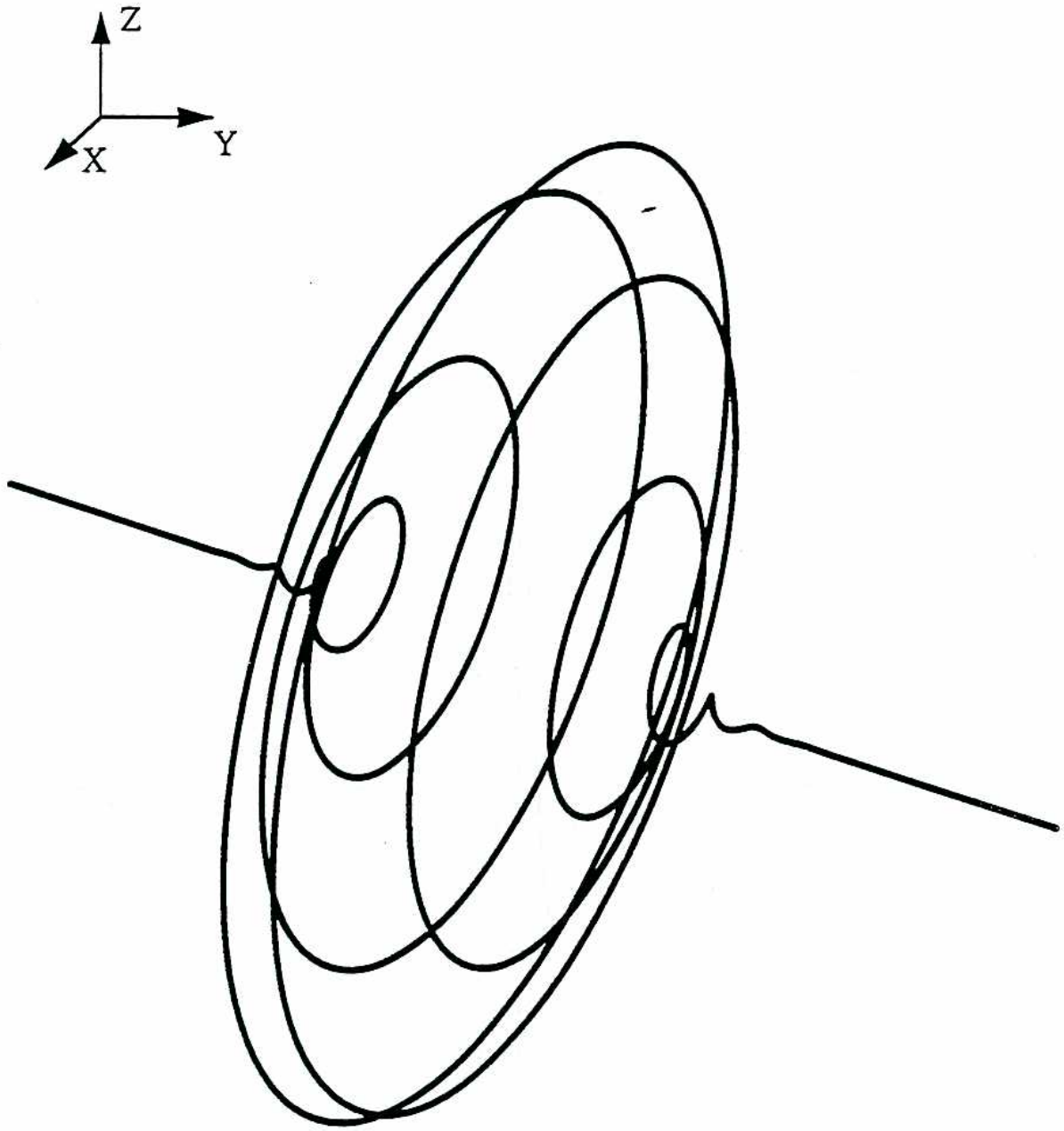

Fig. 4.2

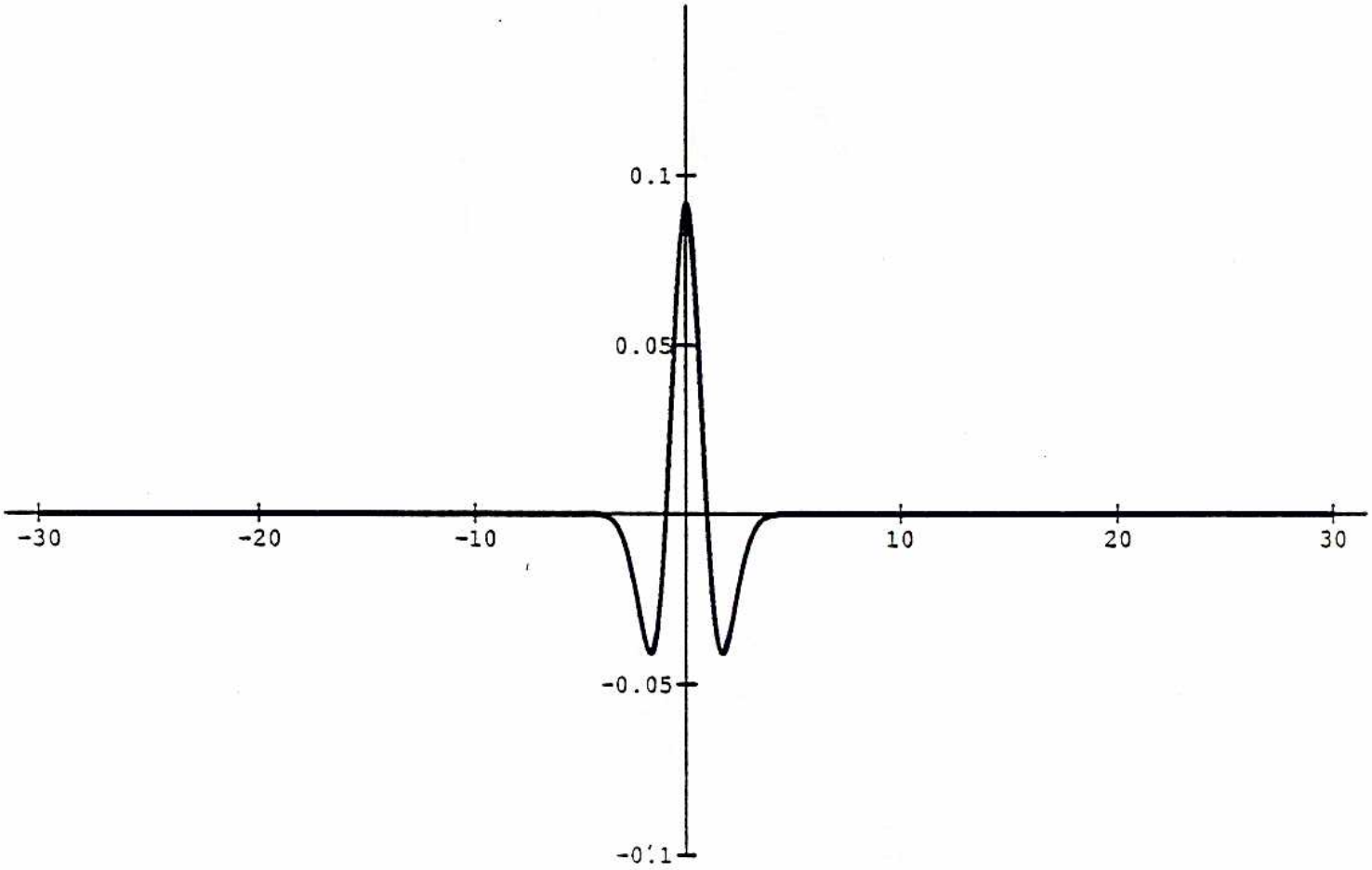

Fig. 4.3a

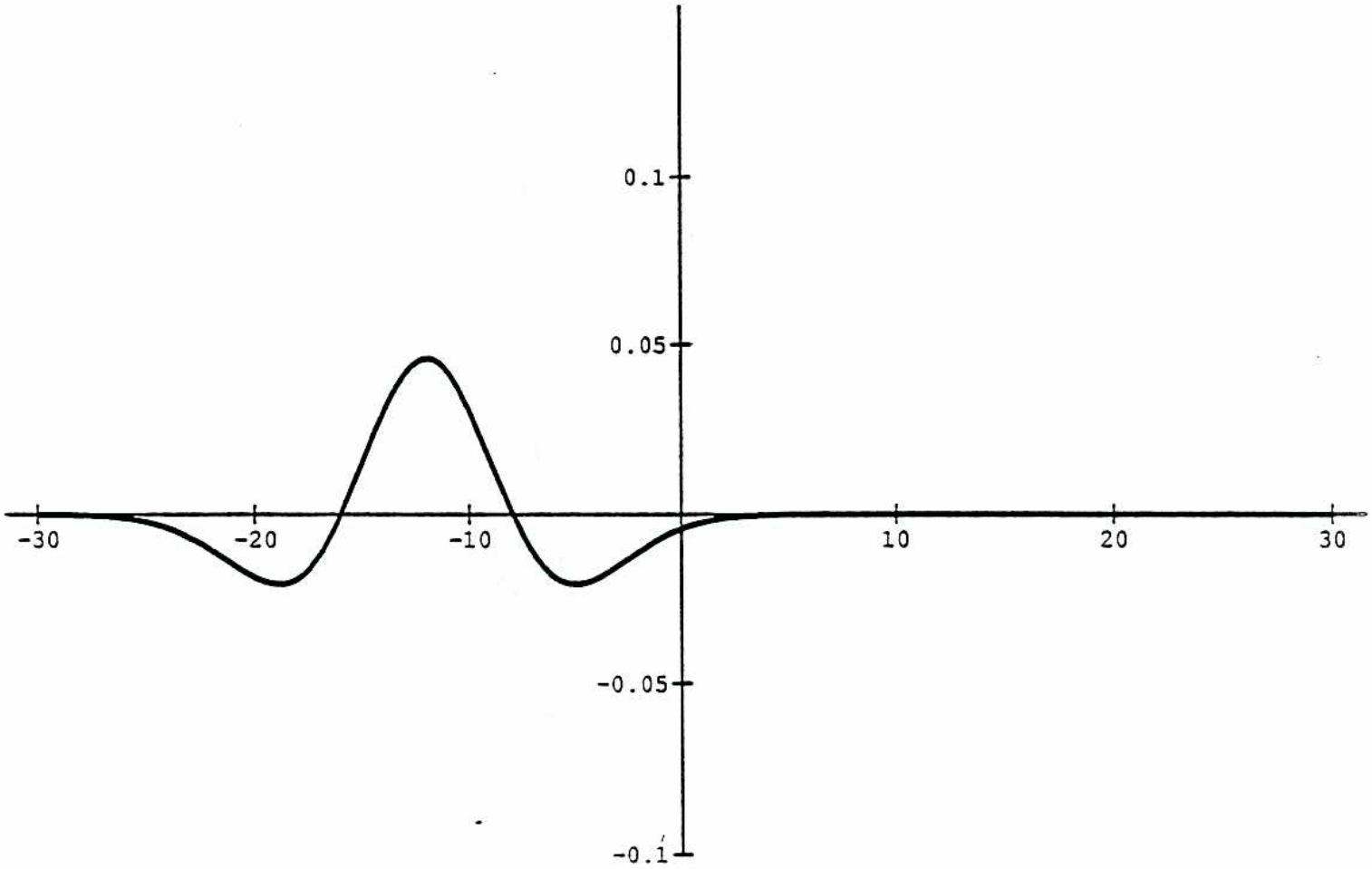

Fig. 4.3b

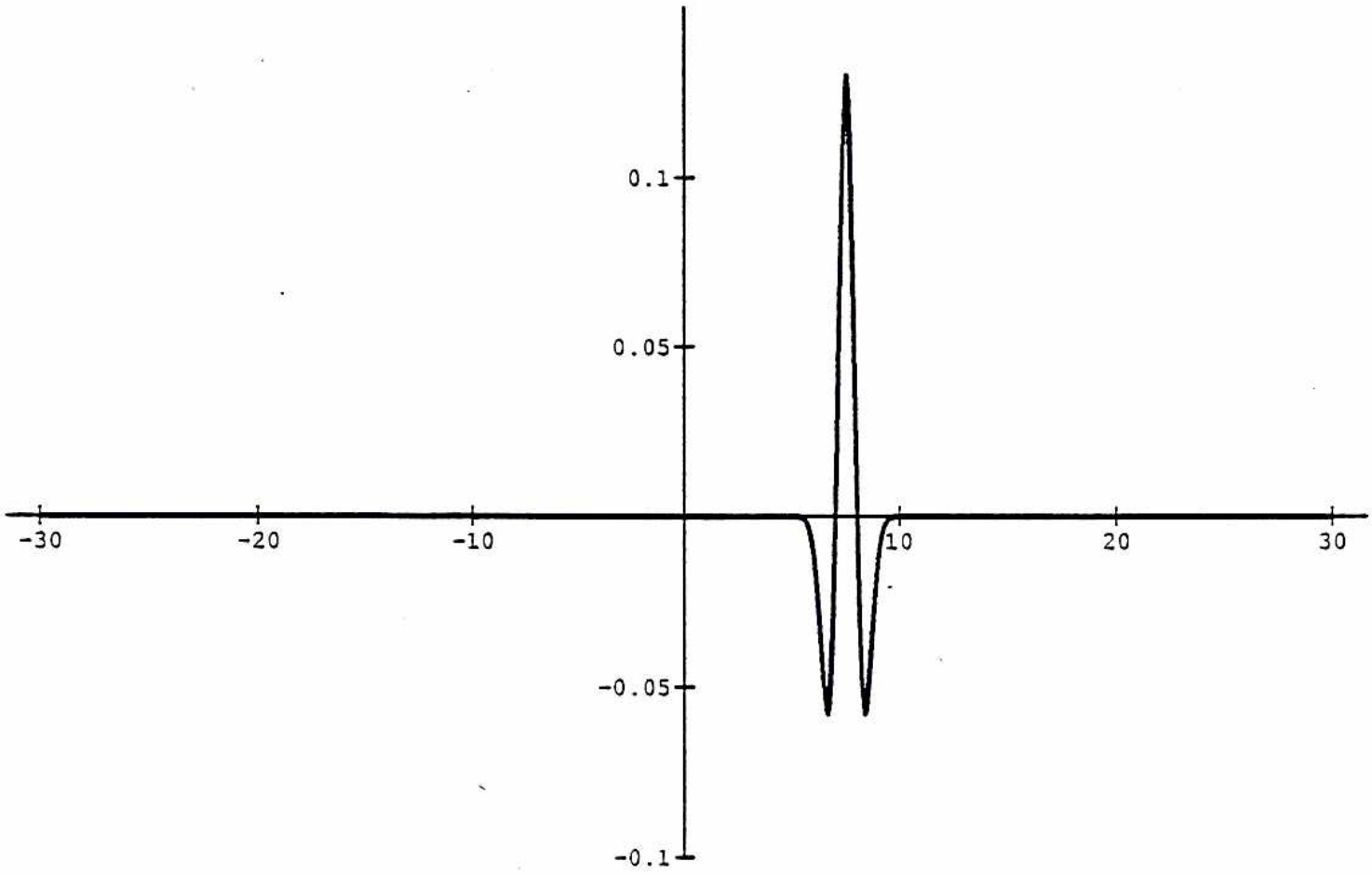

Fig. 4.3c